LA-UR-25-30114

Approved for public release; distribution is unlimited.

Title: Effects of Salt Concentration, Ionic Strength, and Water Activity on the Growth of a WIPP Archaeal Isolate, Halobacterium sp.

Author(s): Swanson, Juliet S.

Intended for: Report

Issued: 2025-10-13

Los Alamos
NATIONAL LABORATORY







Los Alamos National Laboratory, an affirmative action/equal opportunity employer, is operated by Triad National Security, LLC for the National Nuclear Security Administration of U.S. Department of Energy under contract 89233218CNA000001. By approving this article, the publisher recognizes that the U.S. Government retains nonexclusive, royalty-free license to publish or reproduce the published form of this contribution, or to allow others to do so, for U.S. Government purposes. Los Alamos National Laboratory requests that the publisher identify this article as work performed under the auspices of the U.S. Department of Energy. Los Alamos National Laboratory strongly supports academic freedom and a researcher's right to publish; as an institution, however, the Laboratory does not endorse the viewpoint of a publication or guarantee its technical correctness.

ACRSP Cover Sheet

Title:	LCO-ACP-028, Rev 0 - Effects of Salt Concentration, Ionic Strength, and Water Activity on the Growth of a WIPP Archael Isolate, Halobacterium sp.
Originator:	Julie Swanson
ACRSP Document Number:	ACP-17-030
Date Generated:	
Comments:	
Classification:	Lifetime Record submitted to the LANL-CO Record Center: 11-22-22 (Date) (Initial)

Notice: The current controlled version of this document is on the LCODocs website (https://lcodocs.lanl.gov/). A printed copy of the document may not be the current version.

LOS ALAMOS NATIONAL LABORATORY
CARLSBAD OPERATIONS

LCO-ACP-28, Revision 0

Effects of Salt Concentration, Ionic Strength, and Water Activity on the Growth of a WIPP Archaeal Isolate, *Halobacterium* sp.

Effective Date: 11-22-22

Originator:

Julie Swanson, LANL-CO ACRSP — Date: 11-22-22

Technically Reviewed by:

Adrianne Navarrette, LANL-CO ACRSP — Date: 11-22-22

Approved by:

Jeremy Beam, LANL-CO ACRSP Team Leader — Date: 11/22/22

Priscilla Yanez, LANL-CO Quality Assurance Manager — Date: 11/22/2022

Doug Weaver, LANL-CO WIPP/RSO Program Director — Date: 11-22-2022

History of Revisions

Revision Number	Effective Date	Pages Affected	Description of Revision
0	11-22-22	All	Original Release

ACRONYMS AND ABBREVIATIONS

a_w	water activity
Ca^{2+}	calcium ion
CFU	colony-forming units
C/K	chaotrope/kosmotrope ratio
Cl^-	chloride ion
DGR	deep geological repository
DHAB	deep sea hypersaline anoxic brine
ERDA-6	Energy Research and Development Administration Well 6
GWB	Generic Weep Brine
IC	ion chromatography
ICP-MS	inductively-coupled plasma mass spectrometry
K^+	potassium ion
L	liter
Log(C/K)	log of the chaotrope/kosmotrope ratio
M	molar; moles/liter
Mg^{2+}	magnesium ion
mM	millimolar; millimoles/liter
Na^+	sodium ion
OD	optical density
pC_{H+}	negative log of the hydrogen ion concentration
pH	negative log of the hydrogen ion activity
sp.	species (singular)
v/v	volume/volume ratio
w/v	weight/volume ratio
WIPP	Waste Isolation Pilot Plant

EXECUTIVE SUMMARY

An extremely halophilic archaeon (*Halobacterium* sp., WIPP strain), isolated from WIPP halite, was tested for its ability to grow in media containing various combinations of sodium and magnesium chloride that influenced overall ionic strength and water activity. *Halobacterium* sp. grew well in most tested salt combinations, and its growth appeared to depend more upon the relative contribution of sodium to overall ionic strength than on other parameters. Growth rates were highest when media consisted of at least 2 M NaCl and lowest when NaCl dropped below 20% of the ionic strength (usually less than 0.5 M). High magnesium concentrations (1 and 1.5 M $MgCl_2$) did not prevent *Halobacterium* sp. growth, as long as the sodium contribution was sufficient. Water activity was not a definitive factor in determining growth, because this value did not reach an extreme lower limit in the experimental media.

Because the tested parameters are interdependent, it is difficult to say which is the chief determinant affecting the growth of this organism. However, comparisons between these results and those in the literature suggest that growth is possible when a balance is achieved between chaotropic (e.g., Mg^{2+}) and kosmotropic (e.g., Na^{+}) solutes at a permissive water activity and permissive pH. Chaotropic substances cause disruption in cellular structures, while kosmotropic substances can balance these adverse effects. To test this theory, a "C/K index" was calculated as the ratio of chaotropic to kosmotropic solutes in the growth media. This index was also calculated for numerous other hypersaline environments from literature data. Results suggest that a 3-dimensional "window of habitability" can be delineated by the chaotrope/kosmotrope index, water activity, and pH.

In these experiments, this window is defined for halophiles. The fact that an extreme halophile did not grow well, or even at all, in some of the media combinations suggests that a less halophilic organism might not grow at all. This supports the argument that not all organisms will be active under WIPP conditions.

TABLE OF CONTENTS

1.0 INTRODUCTION..... 6

2.0 EXPERIMENTAL METHODS..... 7

2.1 Growth Media..... 7

2.2 Organism..... 8

2.3 Parameters Measured..... 8

2.4 Parameters Calculated..... 9

3.0 RESULTS AND DISCUSSION..... 9

3.1 Organism Growth..... 9

3.2 Cell Morphological Changes..... 16

3.3 Changes in Ion Concentration..... 17

4.0 DISCUSSION AND CONCLUSIONS..... 23

5.0 QUALITY ASSURANCE, DATA TRACEABILITY, AND DOCUMENTATION..... 32

6.0 REFERENCES..... 32

APPENDICES..... 37

1.0 INTRODUCTION

Although microorganisms are present in the Salado Formation, their activity under projected WIPP conditions is far from certain. Even if the potentially adverse effects of radioactivity are disregarded, the presence of high ionic strength, low water activity ($a_w < 0.75$), and high concentrations of chaotropic solutes (i.e., Mg^{2+} or Ca^{2+}) can significantly constrain microbial activity.

Sodium concentration is the primary determinant of microbial community structure in saline settings, with 15%, w/v, NaCl (2.57 M) representing the transition in community composition from moderate to extreme halophiles (Andrei et al., 2012; Kimbrel et al., 2018). Thus, hypersaline environments are dominated by members of the Euryarchaeal Class Halobacteria, because of their ability to use the low energetic cost "salt-in" strategy for osmoregulation. These "haloarchaea" have been the main organisms enriched from cultures of WIPP halite at high salt concentrations and are the main organisms detected from other subterranean halites as well (Vreeland et al., 1998; Vreeland et al., 2007; Swanson et al., 2012; Jaakkolla et al., 2016; Megaw et al., 2019). After salinity, chaotropicity may be the next greatest limiting factor to microbial activity (Hallsworth et al., 2003, 2007; dC Rubin et al, 2017; Lee et al, 2018). High concentrations of chaotropic solutes, such as Mg^{2+} or Ca^{2+}, can destabilize proteins and affect membrane structure (Hallsworth et al., 2003, 2007; Broering and Bommarius, 2008). Finally, low water activity can effectively delimit a habitable zone, even though halophilic microorganisms can do well at low values (Hallsworth et al., 2003; Grant, 2004; Williams and Hallsworth, 2009; Stevenson et al., 2014). These three stressors are interrelated in many hypersaline environments, and they can determine which life forms survive and thrive and which do not.

In spite of these constraints on microbial survival and growth, repository performance simulations must assume that all microorganisms are healthy and active in such environments, in order to predict the worst-case scenario—i.e., the microbially influenced release of radionuclides into the biosphere. A series of experiments is underway to determine the likelihood of survival and growth of organisms isolated from the WIPP environment under various combinations of ionic strength, water activity, sodium concentration, and magnesium concentration, but in the presence of their preferred organic substrates. This report will present data from growth experiments on the first of these organisms, *Halobacterium* sp. This organism was chosen for study because it is an extreme halophile, it is commonly detected in subterranean salt deposits, and it is capable of growth in both WIPP brines, GWB and ERDA-6 (Radax et al., 2001; Gruber et al., 2004; Vreeland et al., 2007; Park et al., 2009; Gramain et al., 2011; Yildiz et al., 2012; Swanson et al., 2012; Jaakkolla et al., 2016; Swanson and Reed, 2018). Therefore, if *Halobacterium* sp. growth is affected, then the survival and growth of less halotolerant organisms is even more uncertain. While pH extremes can also affect microbial growth, they were not considered in the experimental tasks for this work; the assumption is made that the immediate osmotic shock caused by exposure to brines will outweigh the effect of extreme pH.

2.0 EXPERIMENTAL METHODS

2.1 Growth Media

Two series of growth media were prepared—one with constant ionic strength and one with varying ionic strength—according to the table below. Within each series, several variations of NaCl and $MgCl_2$ concentrations were tested. For the purposes of these experiments, the target ionic strengths were only calculated from the summed concentrations of NaCl and $MgCl_2$, since they were the predominant salts added (KCl and $CaCl_2$ contributed less than 0.03 M). Organics were not factored into calculations.

All broths contained the following basal composition, and only the sodium and magnesium salts varied.

Table 1. Growth medium composition (without NaCl and $MgCl_2$).

Medium component	grams/L
KCl	2.00
$CaCl_2 \cdot 2H_2O$	0.20
Yeast extract	2.50
Casamino acids	2.50
Proteose peptone #3	2.50
Sodium pyruvate	0.11
Trisodium citrate	0.26
Trace minerals	1 ml

Broth pH was adjusted to between 6.8-7.3. Values were measured at least twice before starting the experiments, since the pH tended to drift downward with increasing magnesium concentration. To be consistent with the microbiology literature, pH values provided are measured values and are not converted to pC_{H+}.

Table 2. Broth designations, major salt concentrations and pH.

Broth Designation	[NaCl], M	[$MgCl_2$], M	Ionic Strength (NaCl+$MgCl_2$)	Measured pH	Water Activity
3.42-A	3.42	0	3.42	7.29	0.8632
3.42-B	3.12	0.10		7.15	0.8684
3.42-C	2.67	0.25		7.34	0.8761
3.42-D	1.92	0.50		7.24	0.8895
3.42-E	1.17	0.75		7.28	0.9032
3.42-F	0.42	1.00		7.18	0.9176
3.42-G	0	1.15	3.45	7.31	0.9251
5-A	5.00	0	5.00	7.22	0.7762
5-B	4.25	0.25		7.20	0.7900

5-C	3.50	0.50		7.16	0.8039
5-D	2.75	0.75		7.29	0.8177
5-E	2.00	1.00		7.11	0.8317
5-F	1.25	1.25		7.15	0.8462
5-G	0.50	1.50		7.13	0.8612
5-H	0	1.67		7.13	0.8711
1-A	0	1.0	3.0	7.00	0.9380
1-B	0.5		3.5	7.04	0.9136
1-C	1.0		4.0	7.05	0.8878
1-D	1.5		4.5	7.01	0.8606
1-E	2.0		5.0	7.00	0.8319
1-F	2.5		5.5	6.96	0.8015
1-G	3.0		6.0	6.96	0.7696
1.5-A	0	1.5	4.5	6.91	0.8903
1.5-B	0.5		5.0	6.91	0.8611
1.5-C	1.0		5.5	6.92	0.8306
1.5-D	1.5		6.0	6.87	0.7986
1.5-E	2.0		6.5	6.99	0.7654
1.5-F	2.5		7.0	6.88	0.7307
1.5-G	3.0		7.5	6.80	0.6984
2-A	0	2.0	6.0	6.96	0.8294
2-B	0.5		6.5	6.91	0.7955
2-C	1.0		7.0	6.88	0.7606
2-D	1.5		7.5	6.85	0.7244
2-E	2.0		8.0	6.82	0.6873

2.2 Organism

Halobacterium sp. was originally isolated from WIPP halite at 4.71 M NaCl (Swanson et al., 2012). For these experiments, it was grown in generic halophile broth (Table 1) containing its optimum formula with 3.42 M NaCl and 0.1 M $MgCl_2$. At late log/early stationary phase, *Halobacterium* sp. was subcultured (2% v/v) into triplicate tubes containing broth from each series (Table 2).

2.3 Parameters measured

2.3.1 Growth

Growth was measured as the optical density (OD) at 660 nm using a GeneSys 50 spectrophotometer. The growth rate, k, was calculated as the change in OD during exponential growth and is calculated in units per day for this organism:

$k = (OD_{t2}-OD_{t1})/(t_2-t_1)$, where

t_1 and t_2 are the times at which exponential growth begins and ends, respectively.

Optical density readings were periodically confirmed by plating for colony-forming units (CFU) onto agar media with the same formulation as the broth and the optimum NaCl concentration and by direct microscopic counts. Cells were stained with the LIVE/DEAD® BacLight™ nucleic acid stain prior to visualization with a Zeiss Axioscope 40 fluorescence microscope. Cells/ml (N) were calculated as follows (Kepner and Pratt, 1994):

$N = (N_f A)/(aV)$, where

N_f = cells counted per microscopic field examined

A = area examined (approximate area of coverslip)

V = volume corrected for dilution

a = area of microscopic field (at 1000X magnification)

2.3.2 Ion concentrations

Cation (Na^+, Mg^{2+}, K^+, and Ca^{2+}) concentrations in the growth media were verified using an Agilent 7900 inductively-coupled plasma mass spectrometer (ICP-MS; Santa Clara, CA). Calibration curves were generated from a commercial standard cation mix (High Purity Standards; Charleston, SC), and indium was used as the internal standard. Chloride concentrations were measured on a Dionex Ion Chromatography System (ICS)-6000 (ThermoFisher Scientific; Waltham, MA) with conductivity detection and also calibrated with a commercial standard anion mix (High Purity Standards). These constituents were measured before inoculating the media and again at stationary phase, to determine if ion concentrations changed during cell growth.

2.4 Parameters calculated

Water activities and overall ionic strengths (all ions, not just Na^+ and Mg^{2+}) were calculated with the SpecE8 application in Geochemist's Workbench version 14.0, using the Pitzer thermodynamic database, FMT4 (Domski, 2020). Activities of broths were calculated at the experimental incubation temperature (37°C), as temperature affects both water activity and chaotropicity. Organic components were not included in these calculations. Geochemist's Workbench calculations cannot be considered Quality Level 1 data, since the software has not been formally qualified, although it is used extensively in the field of geochemistry. Therefore, calculations were validated using the FMT4 database in EQ3/6 software (Wolery, 1992).

3.0 RESULTS AND DISCUSSION

3.1 Organism Growth

3.1.1 Constant Ionic Strength

In the 3.42 M series, *Halobacterium* sp. grew well with magnesium concentrations between 0-0.2 M $MgCl_2$, but growth slowed with increasing magnesium concentration (Figure 1). In the 5 M series, the fastest growth was observed between 0.25-0.75 M $MgCl_2$, but the overall extent of

growth in the 0 M and 1 M $MgCl_2$ incubations eventually reached the same level as at lower $MgCl_2$ concentrations, suggesting that additional time was necessary for the organism to either osmoregulate or conserve enough energy, after osmoregulation, for actual growth. Little to no growth was observed at higher $MgCl_2$ concentrations (Figure 2).

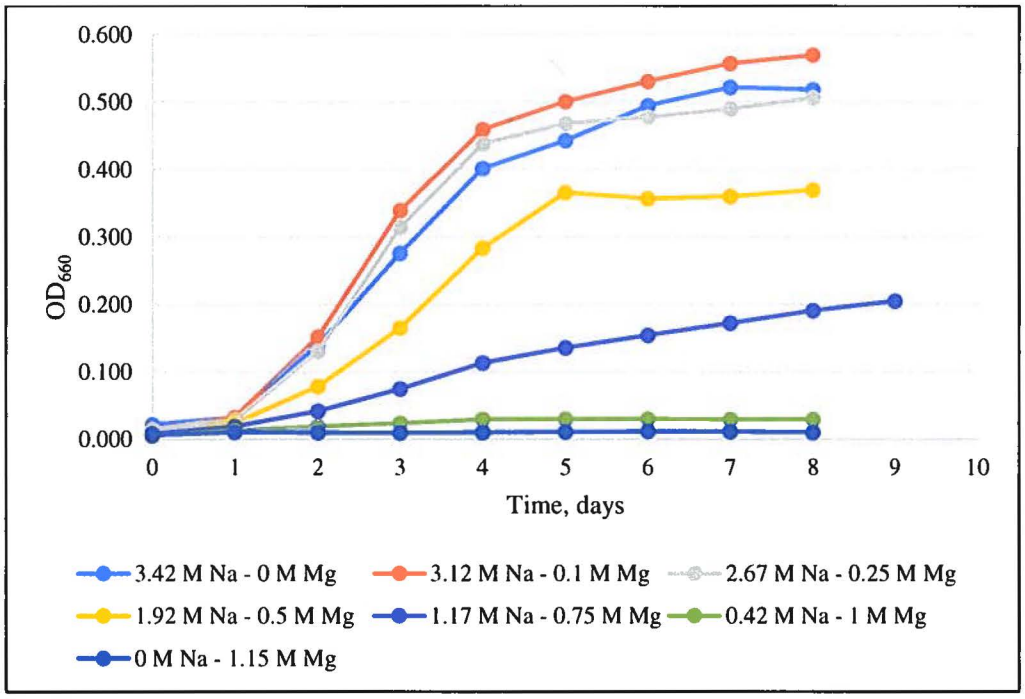


Figure 1. *Halobacterium* sp. growth in the 3.42 M series broths.

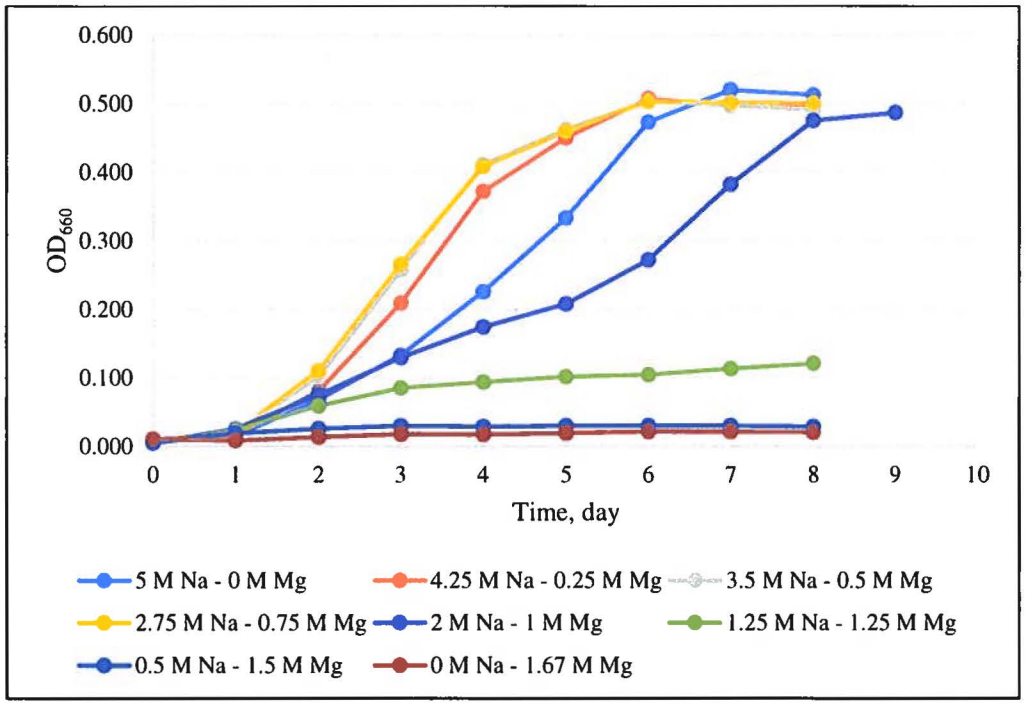


Figure 2. *Halobacterium* sp. growth in the 5 M series broths.

3.1.2 Variable Ionic Strength

In the variable ionic strength series of experiments, the concentration of $MgCl_2$ remained constant within each series (1 M, 1.5 M, 2 M $MgCl_2$), while the NaCl concentration varied. In the 1 M and 1.5 M $MgCl_2$ series, *Halobacterium* sp. grew best when NaCl concentrations were 2 M and above (Figures 3 and 4). Thus, as Mg^{2+} increases, more Na^+ is needed to counter its chaotropic effects, but it is only effective up to a certain point. In the 2 M Mg^{2+} series, 2 M NaCl was the highest concentration used, due to precipitation at higher concentrations (Figure 5). Again, growth was best at this concentration, albeit very slow and with a much lower resulting biomass than at lower Mg^{2+} concentrations (note relative axis scale).

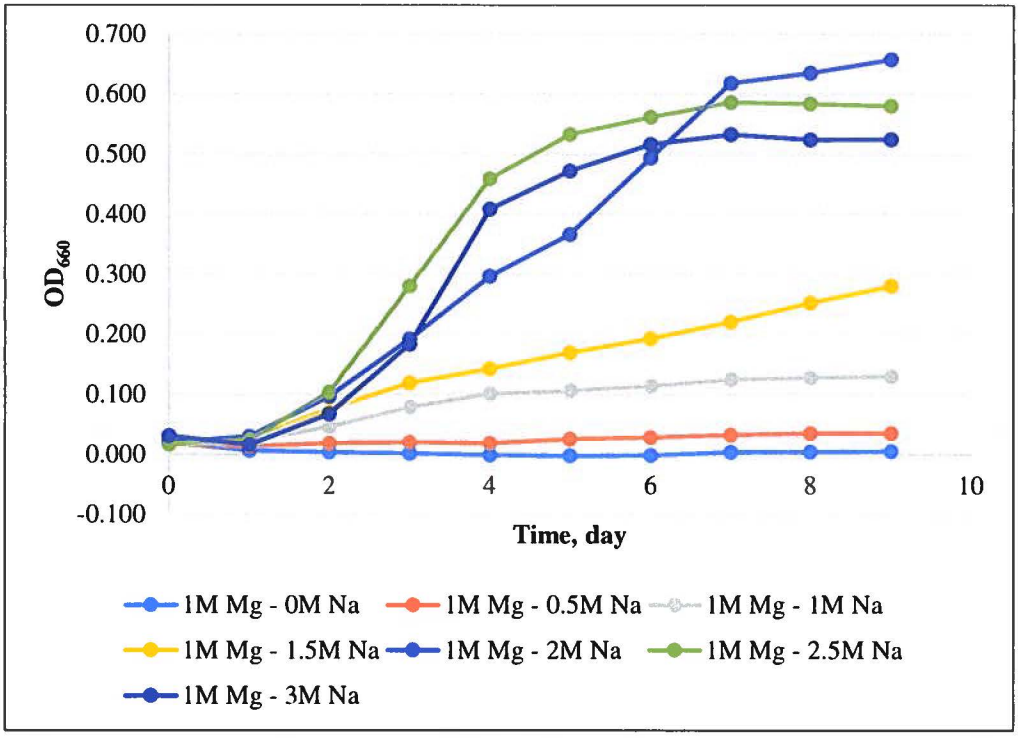


Figure 3. *Halobacterium* sp. growth in broths with 1 M Mg^{2+} and varying Na^+.

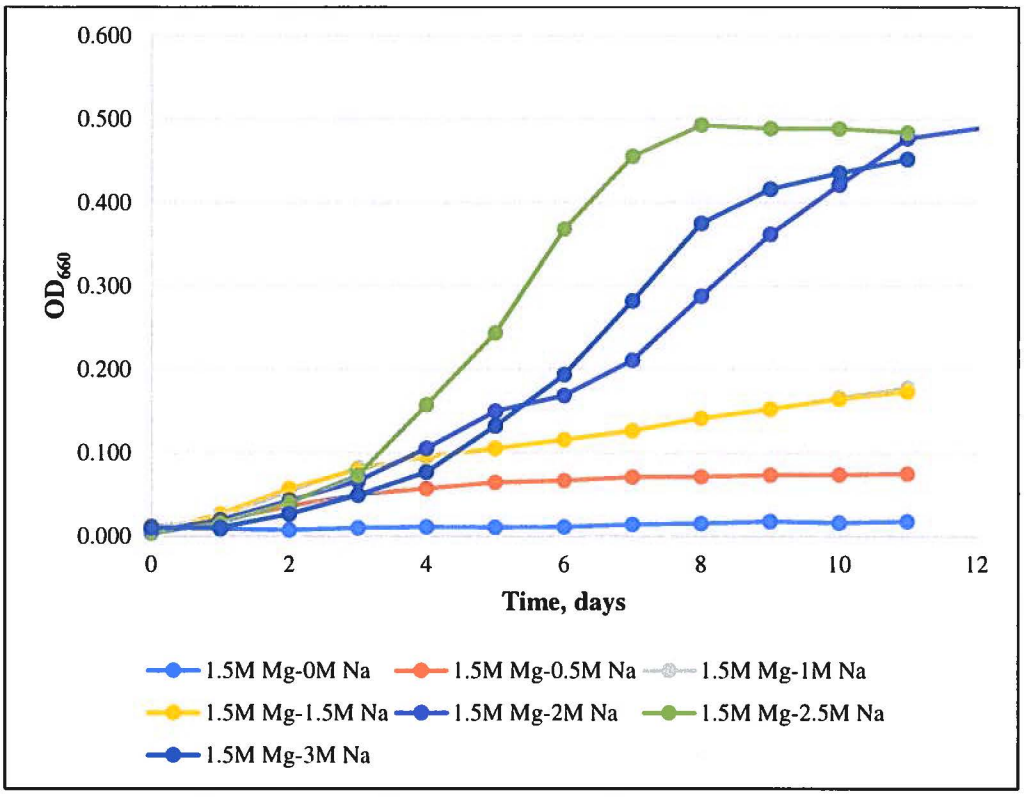


Figure 4. *Halobacterium* sp. growth in broths with 1.5 M Mg^{2+} and varying Na^{+}.

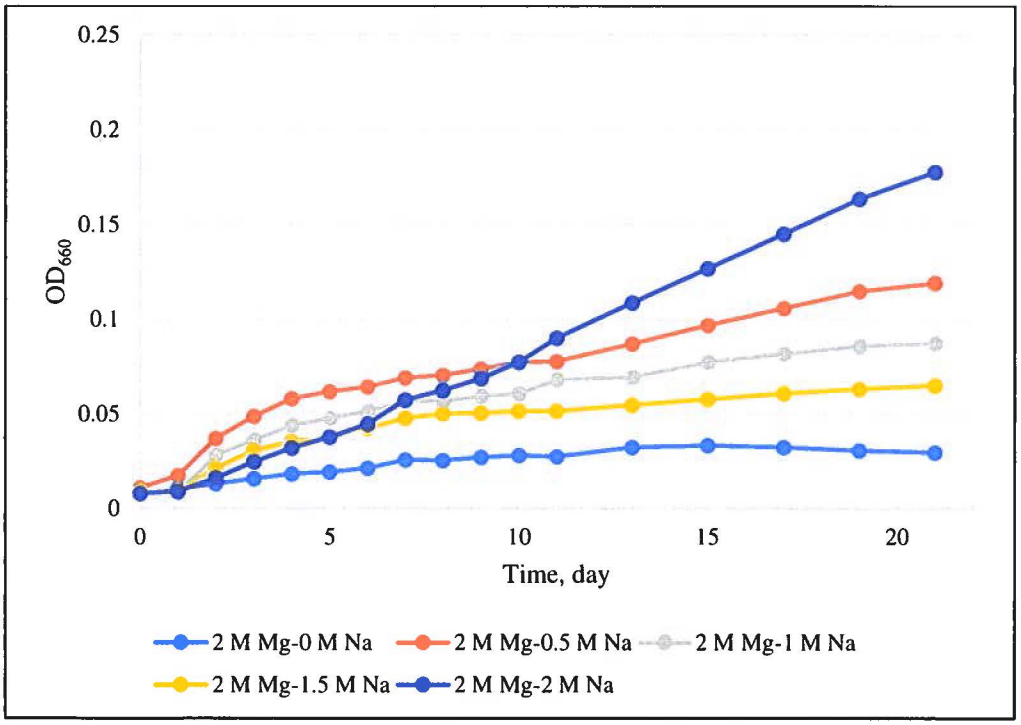


Figure 5. *Halobacterium* sp. growth in broths with 2 M Mg^{2+} and varying Na^{+}.

3.1.3 Comparison of Growth Rates and Extent of Growth

Growth rates and the overall extent of growth (as represented by the maximum optical density value reached) were compared for all conditions (Appendix A; Figures 6 & 7). Growth rates increased with increasing NaCl concentration, for all but the 2 M Mg^{2+} series, but only up to a certain point (~2.5 M NaCl) at which they began to decrease. Maximum OD followed the same trend: an increase in OD with increasing [NaCl] up to a certain point (2 M NaCl) beyond which values decreased. The exception is the 5 M constant ionic strength series, where the rate plateaued between 2.75-4.25 M NaCl (0.75-0.25 M Mg^{2+}, respectively) before decreasing.

In the 1 M and 1.5 M Mg^{2+} series, *Halobacterium* sp. grew faster at 2.5 M NaCl, but maximum biomass occurred at 2 M NaCl. The reason for this is unknown. In broth H of the 5 M constant ionic strength series (no magnesium added), growth was slow but the overall biomass reached was as high as in the other broths. In the 2 M Mg^{2+} series, it was difficult to determine if growth was exponential, especially in the 0 Na^+ and 2 M Na^+ curves, which appear almost linear. This will be discussed later.

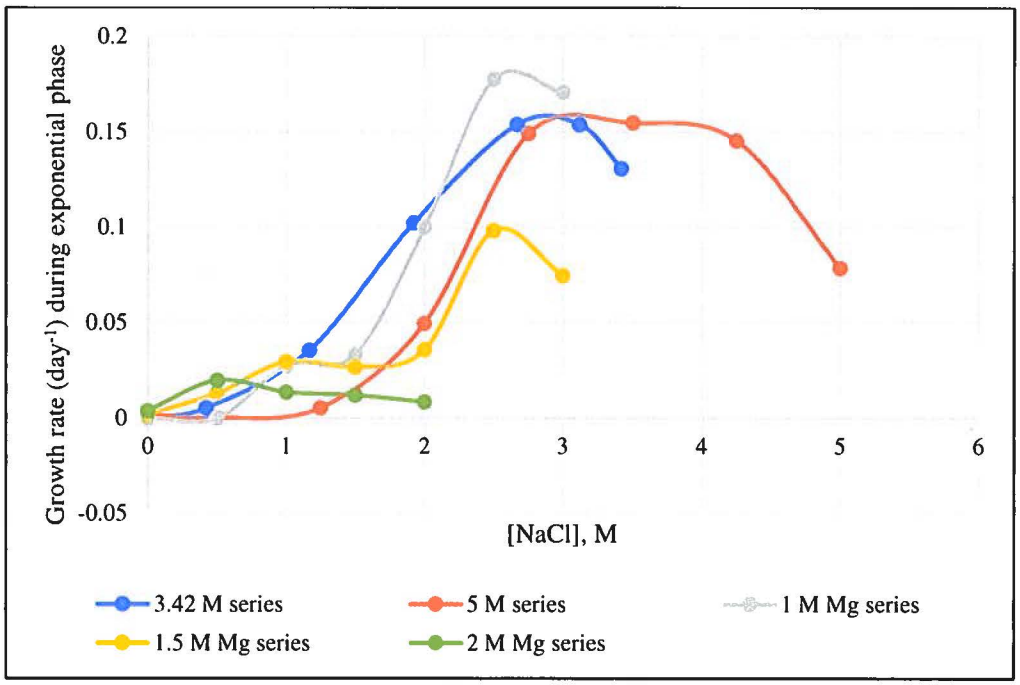


Figure 6. Growth rates of *Halobacterium* sp. within each broth series, as a function of NaCl concentration.

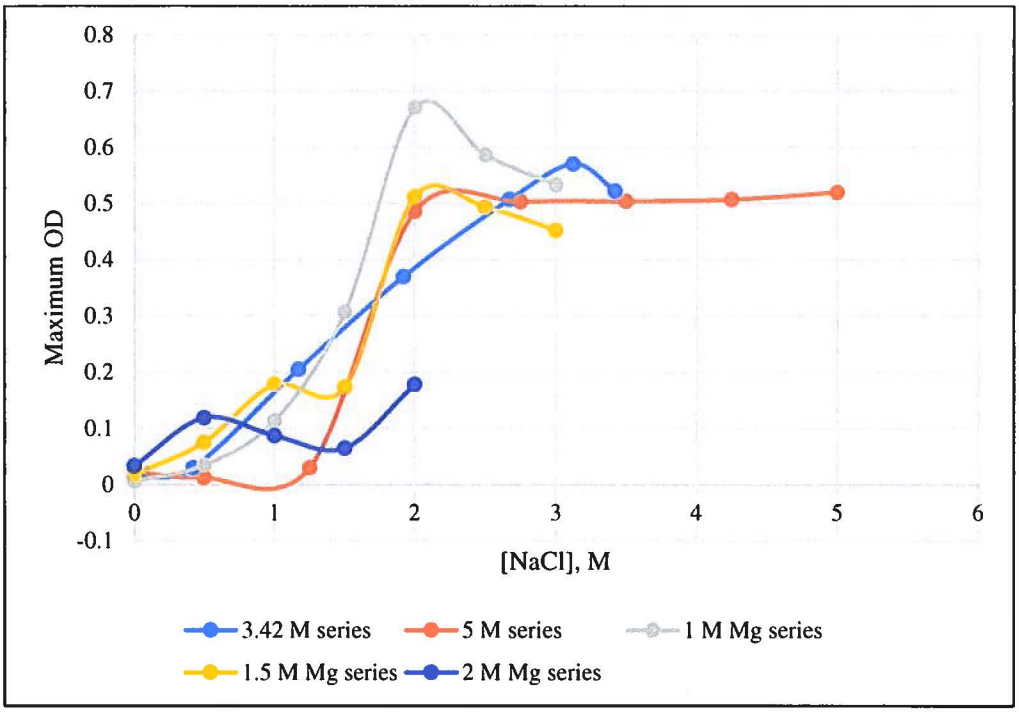


Figure 7. Overall extent of growth, as represented by the maximum OD reading, of *Halobacterium* sp. within each broth series as a function of NaCl concentration.

Growth rates and the extent of growth also increased with decreasing water activities but only to a certain point, at which rates began to decrease (Figures 8 and 9). The difference between the 3.42 M and 5 M series was not significant. However, there was an obvious difference between the magnesium series: growth rates decreased significantly with increasing magnesium, even when water activities were similar.

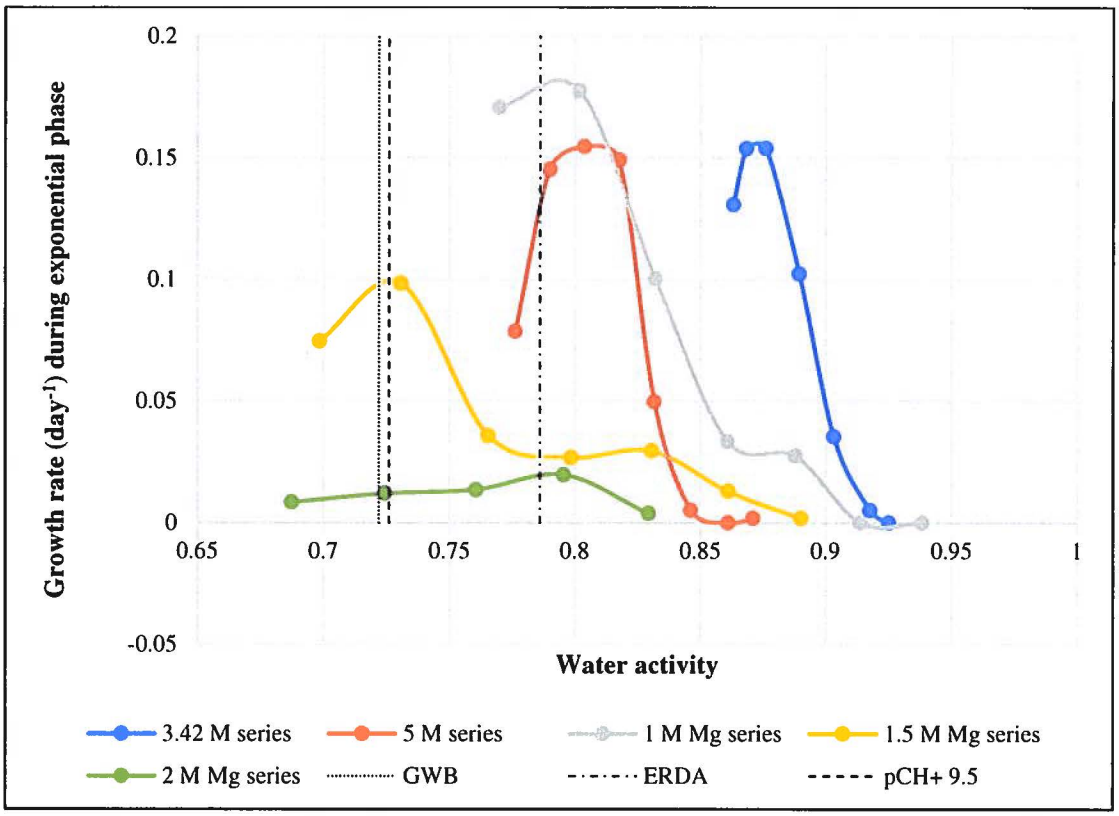


Figure 8. Growth of *Halobacterium* sp. as a function of water activity for each broth series. Dashed lines denote calculated water activities of GWB, ERDA, and pC_{H+} 9.5 brines given for comparison (0.722, 0.786, and 0.726, respectively).

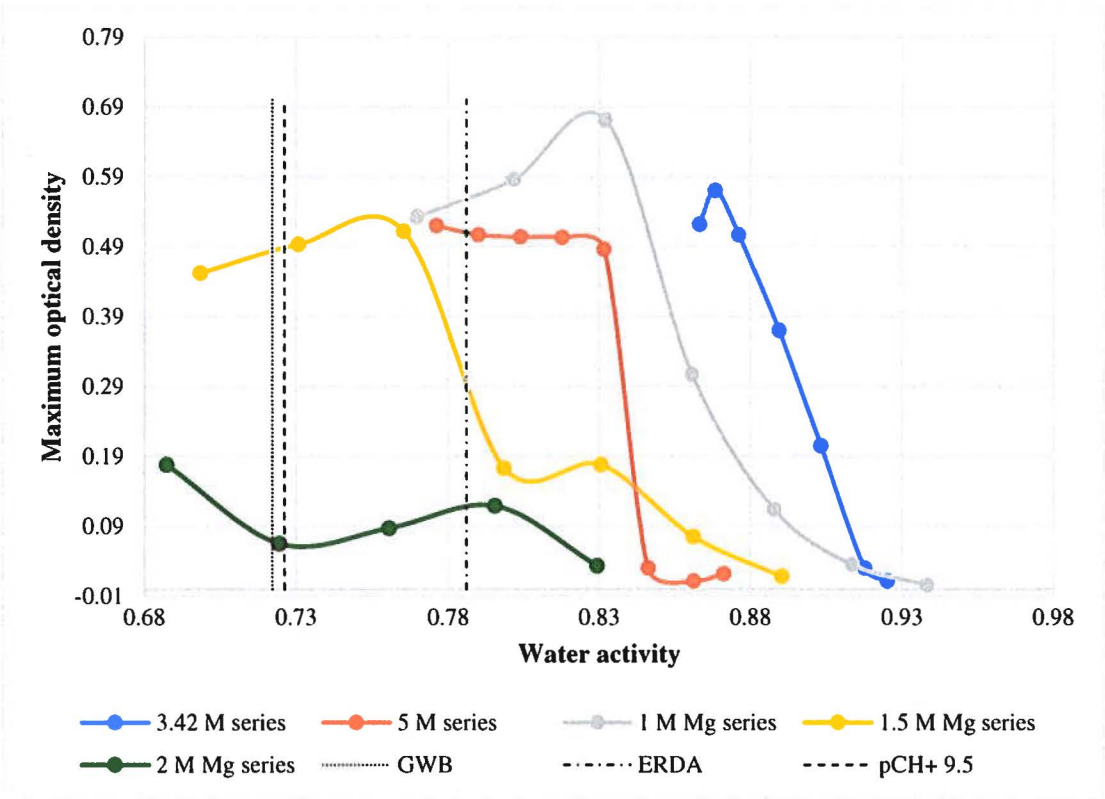


Figure 9. Extent of growth as a function of water activity.

3.2 Cell morphological changes

Rounding up and enlargement of cells was observed in the 1M Mg^{2+} series at all Na^{+} concentrations below 2 M (Figure 10). Below 0.5 M Na^{+}, as sodium concentration increased, so did cell size (Figure 11 from older experiment series). The 2.5 M and 3 M Na^{+} series of replicates resulted in rod shapes. At 2.5 M Na^{+}, the rods were of varying lengths from coccobacilli to long bacilli, and at 3 M Na^{+}, the rods were very long and narrow. *Halobacterium* sp. can be pleomorphic—i.e., can present different morphologies under different environmental conditions—but it usually takes on a rod shape under ideal conditions. When grown in WIPP brines, cells are small and ovoid (coccobacilli).

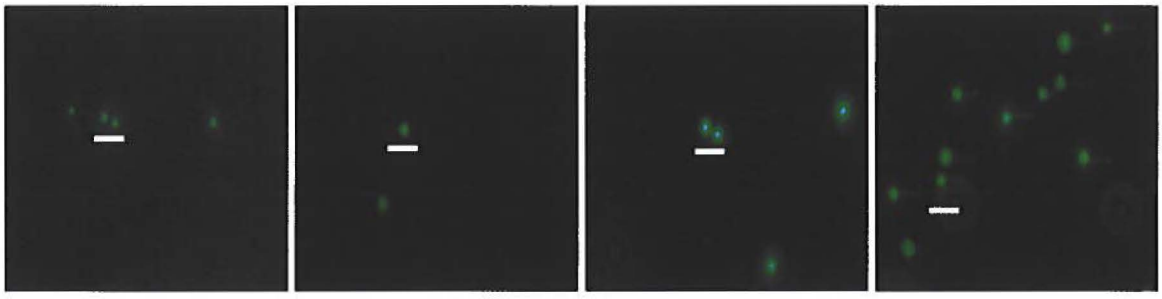


Figure 10. *Halobacterium* sp. cells in the 1 M Mg^{2+} series, from left to right: 0 Na^{+}, 0.5 M Na^{+}, 1 M Na^{+} and 1.5 M Na^{+}. Scale bar denotes 10 microns.



Figure 11. Images showing increasing diameter of *Halobacterium* cells as a function of sodium concentration in 1.5 M Mg^{2+} with low Na^{+} concentrations.

Rounding up has been observed for other species of haloarchaea when exposed to low concentrations of sodium (Abram and Gibbons, 1961; Mohr and Larsen, 1963) or divalent cations, such as magnesium or calcium (Cohen et al., 1991). In those cases, when cation levels dropped too low, the S (surface)-layer was destabilized and often shed, resulting in changes to cell shape.

Lower water activities have been shown to cause rod-shaped *Halobacterium* cells to divide into smaller spherical cells (~0.4 micron in diameter) with a concomitant loss of S-layer surface proteins and a decrease in total surface area (Abram and Gibbons, 1961; Fendrihan et al., 2012). This was proposed as a long-term survival mechanism for these organisms and is not true cell growth. It is possible that the loss of turgor and morphological changes observed in these studies are due to the loss of the S-layer and subsequent inability to maintain cell shape. It is also possible that increases in OD and cell numbers at the highest magnesium concentrations were due to cell splitting and miniaturization instead of true cell division and growth.

Regardless of the cause for morphological change, the change in surface area and the loss of the surface protein S-layer can affect metal or actinide biosorption. S-layer loss and dispersal or decrease in cell surface area could have been the reason for little to no bioassociation of neodymium observed with *Halobacterium* sp. in GWB and pC_{H+} 9.5 brines, due to their high Mg^{2+} content (Swanson, 2019). In comparison, bioassociation in ERDA did occur, albeit more slowly than for similarly tested bacteria.

3.3 Changes in ion concentration

Principal ions (Na^{+}, Mg^{2+}, Cl^{-}, K^{+}, and Ca^{2+}) were measured in the growth media prior to starting the experiments and at the end of cell growth (Figures 12-18). They were also analyzed in the negative controls at the same time point as the final biotic samples were taken. In some instances, there were notable increases in the ion concentrations of uninoculated broths during the course of the experiments (see especially 5 M series, Figure 13). In other cases, ion concentration decreased (see Na^{+} and Mg^{2+} in the 1.5 M Mg^{2+} series-Figure 15; see also Ca^{2+} in the 2 M Mg^{2+} series-Figure 16). Increases in concentration (in uninoculated broths) are thought to be due to enhanced solubility of medium components over time at elevated temperature, while decreases in concentration are due to precipitation with time.

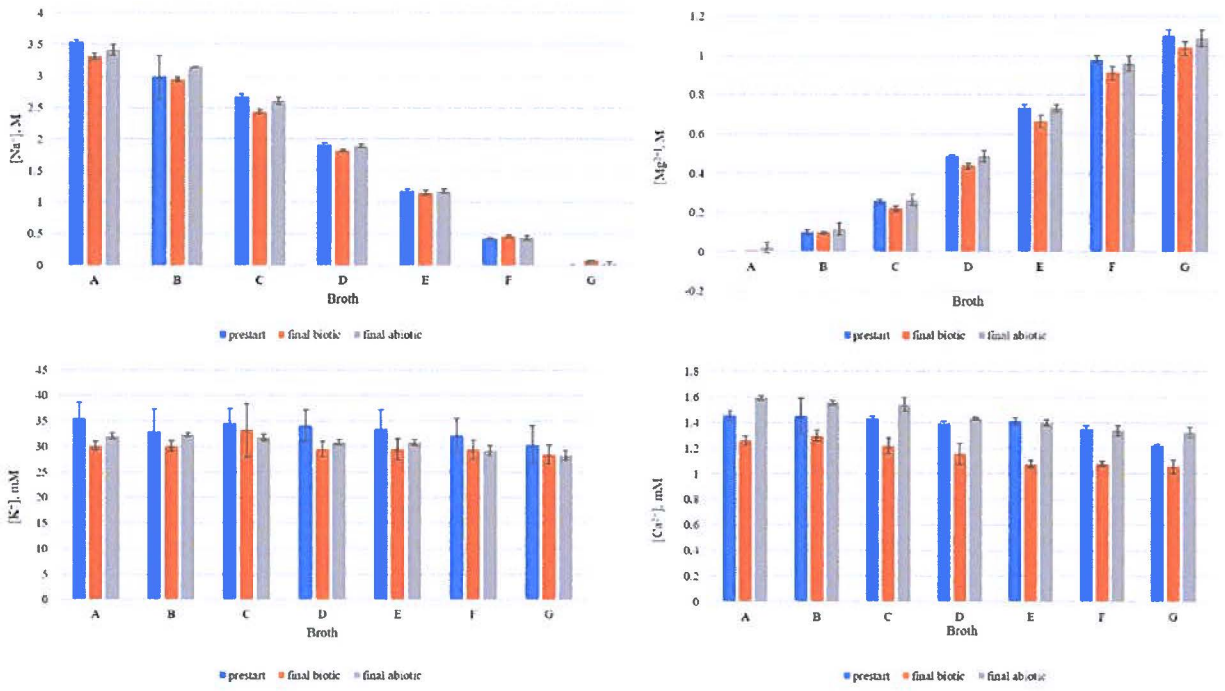


Figure 12. Cation concentrations in 3.42 M constant ionic strength broths before inoculation (prestart) and at the final timepoint (final biotic, final abiotic).

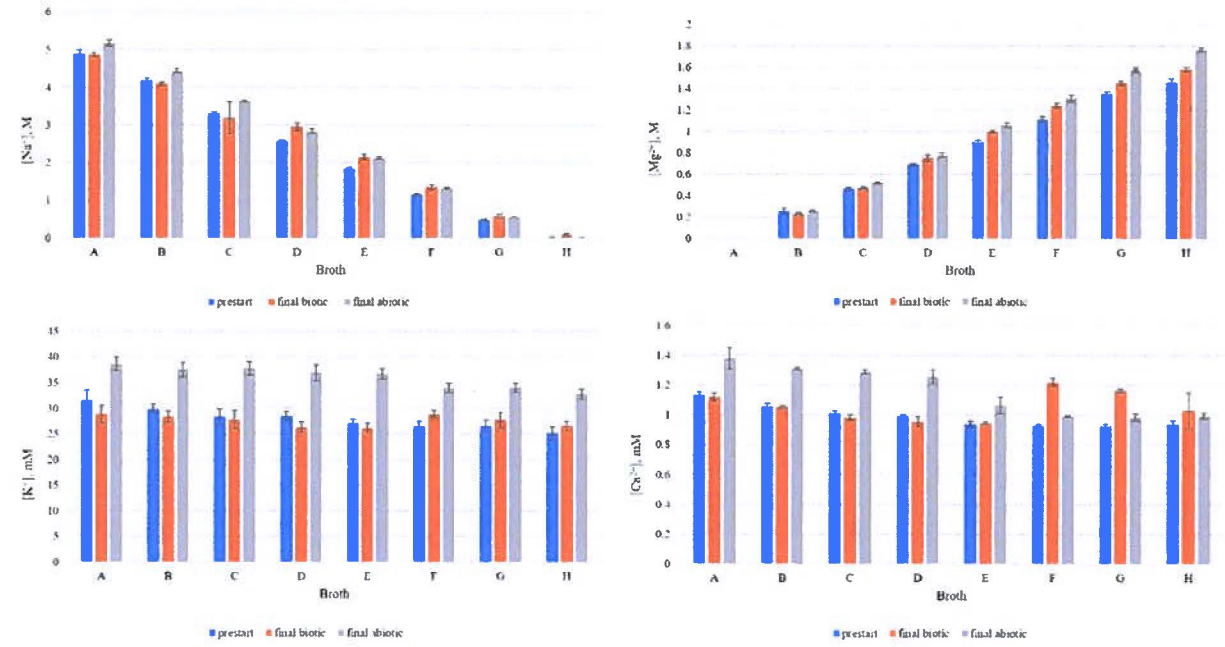


Figure 13. Cation concentrations in 5 M constant ionic strength broths before inoculation (prestart) and at the final timepoint (final biotic, final abiotic).

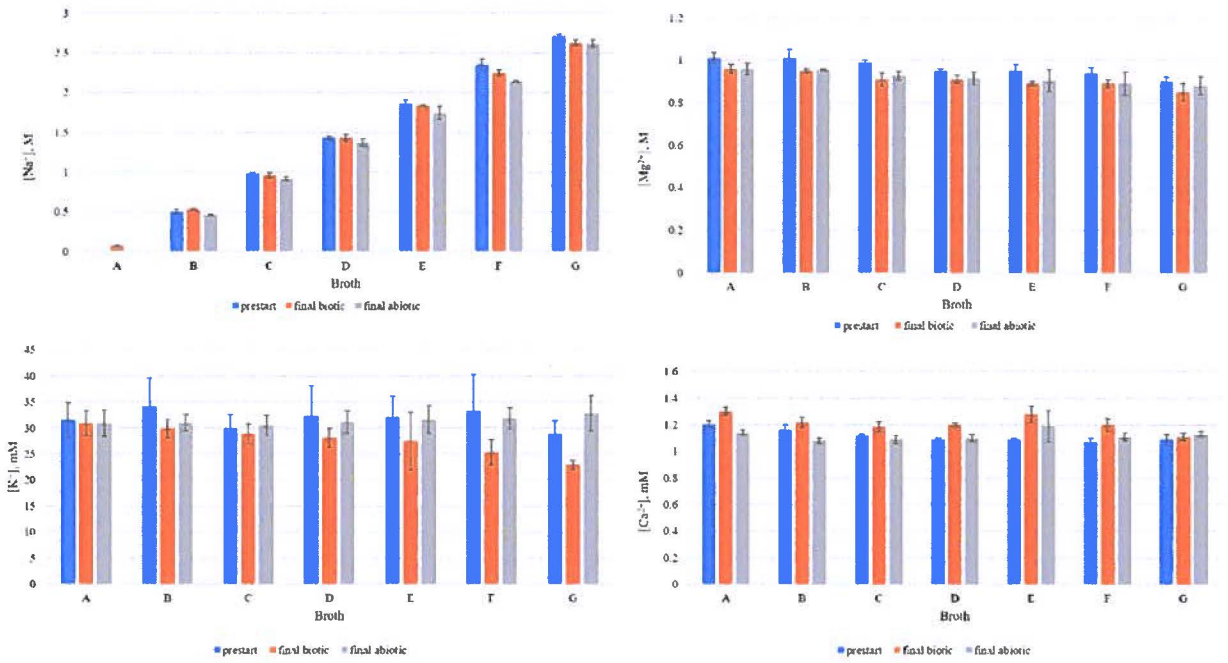


Figure 14. Cation concentrations in 1 M Mg^{2+} variable ionic strength broths before inoculation (prestart) and at the final timepoint (final biotic, final abiotic).

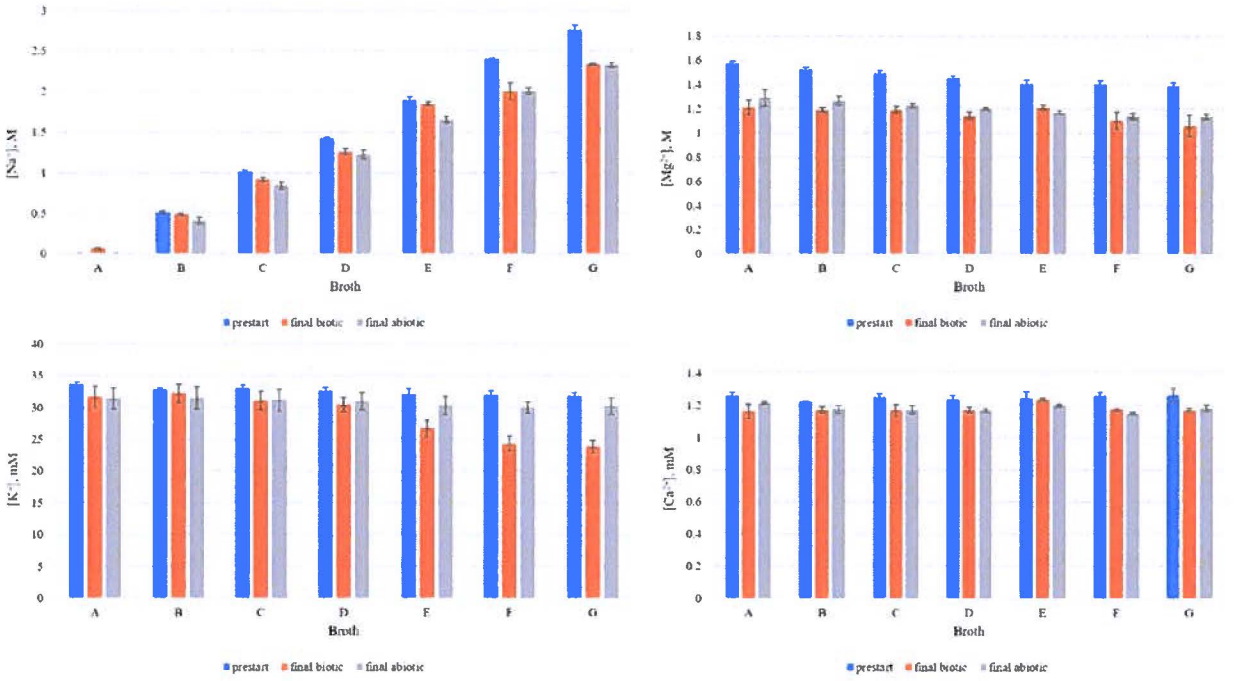


Figure 15. Cation concentrations in 1.5 M Mg^{2+} variable ionic strength broths before inoculation (prestart) and at the final timepoint (final biotic, final abiotic).

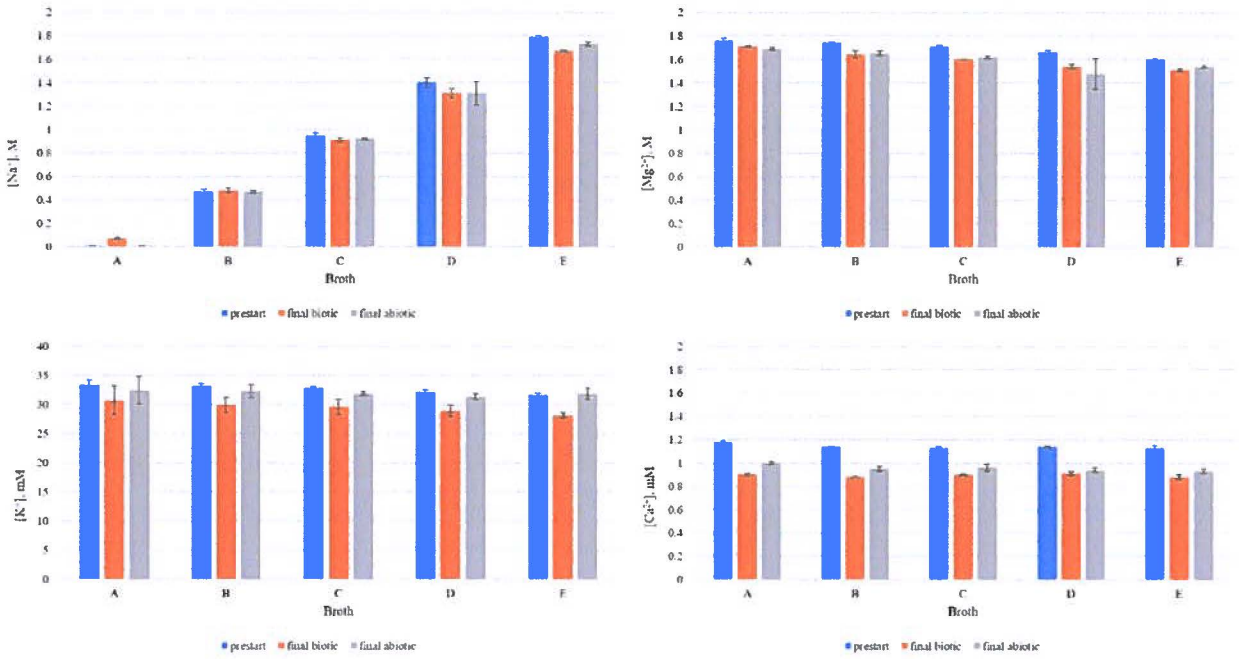


Figure 16. Cation concentrations in 2 M Mg^{2+} variable ionic strength broths before inoculation (prestart) and at the final timepoint (final biotic, final abiotic).

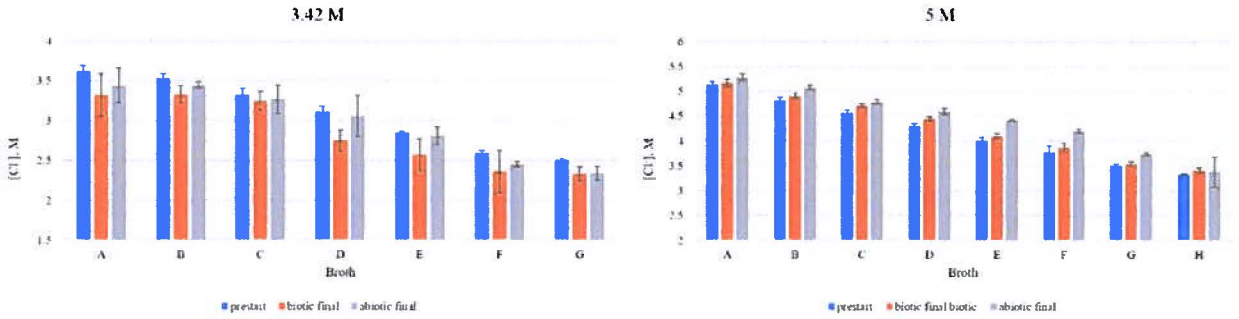


Figure 17. Chloride concentrations in 3.42 M and 5 M constant ionic strength broths before inoculation (prestart) and at the final timepoint (final biotic, final abiotic).

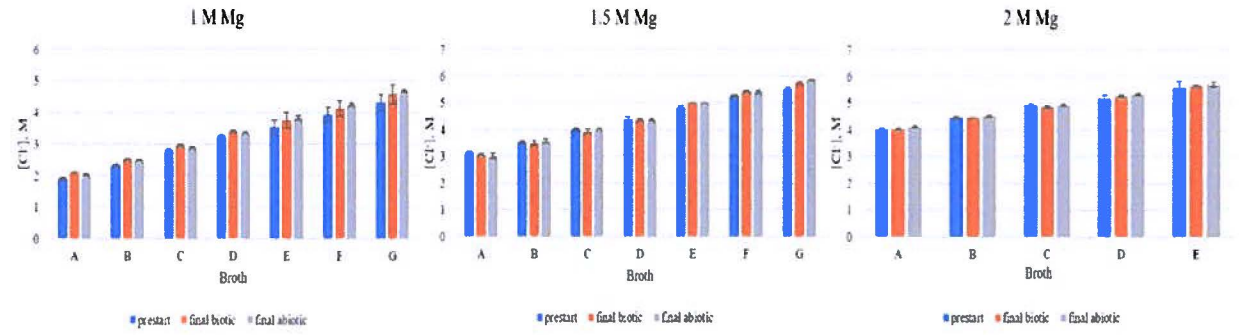


Figure 18. Chloride concentrations in variable ionic strength broths before inoculation (prestart) and at the final timepoint (final biotic, final abiotic).

Because of the differences between prestart and final concentrations for some broths, only final biotic and abiotic sample concentrations were compared. The percent change in ion concentration was calculated as:

$$\%\ change\ in\ ion\ concentration = \left[\frac{ion\ concentration\ in\ final\ abiotic\ supernatant\ -\ ion\ concentration\ in\ final\ biotic\ supernatant}{ion\ concentration\ in\ final\ abiotic\ supernatant}\right] x\ 100$$

Positive values suggest either ion uptake into cells or induced precipitation; negative values represent efflux. It is not possible to determine which process is taking place when a positive value is calculated.

No significant changes were observed in Na^+, Mg^{2+}, or Cl^- concentrations. However, the concentrations of these ions were so high, that it is possible that changes were within the margin of error. In contrast, because calcium concentrations were so low, it was difficult to discern if changes were significant even though trends were observed.

The most important observations were for K^+. Potassium is necessary for *Halobacterium* to maintain osmotic balance, and it can be accumulated intracellularly up to molar levels. Therefore, it is most likely that K^+ loss from the medium was due to uptake and not precipitation. In the 3.42 M constant ionic strength series, there was no measurable difference in K^+ concentrations between biotic samples and abiotic controls (Figures 12, 19, 20). This is likely because the ionic strength in these broths was not high enough to warrant additional uptake for osmoregulation. In the 5 M constant ionic strength series, there was a 20% change in K^+ that increased to almost 30% at 2 M Na^+ (Figures 13, 19, 20). However, in this broth series, there was a significant difference between the prestart and final abiotic concentrations, so it is also possible that the changes in K^+ are an artefact. In the variable ionic strength series, the change in K^+ increased with increasing sodium and decreasing water activity (Figures 14, 19, 20).

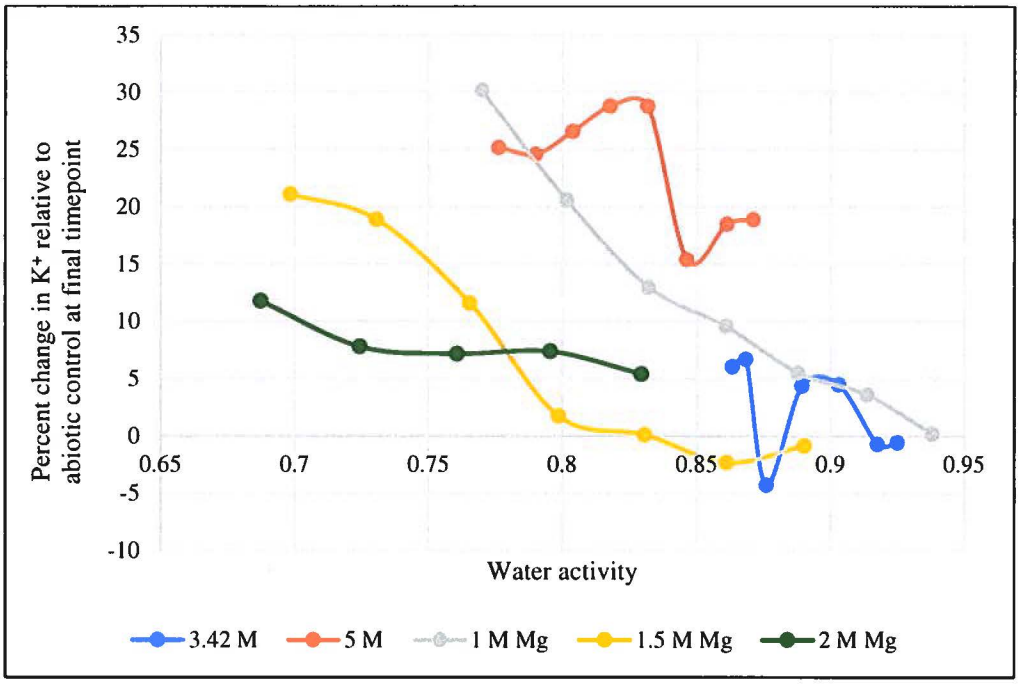


Figure 19. Percent change in potassium concentration of the supernatant as a function of water activity.

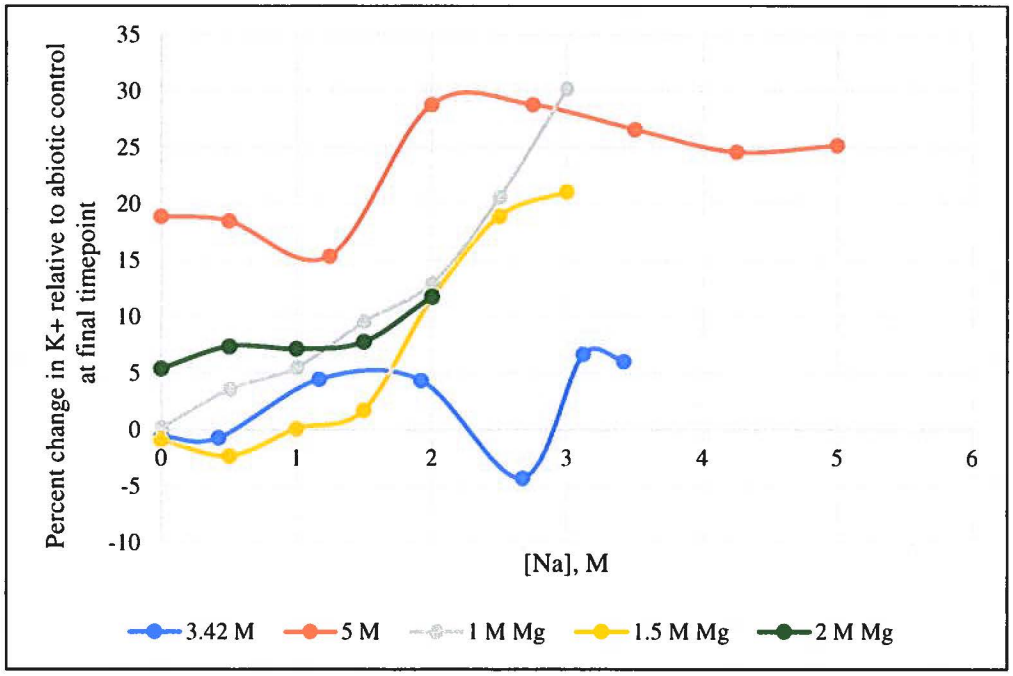


Figure 20. Percent change in potassium concentration in the supernatant as a function of NaCl concentration.

4.0 DISCUSSION AND CONCLUSIONS

Sodium concentration, magnesium concentration, ionic strength and water activity are interdependent parameters in many hypersaline settings, including the WIPP repository, making it difficult to determine which single parameter has the most impact on halophile viability and activity. Even so, *Halobacterium* sp. growth correlated best with the contribution of sodium to the ($Na^+ + Mg^{2+}$) ionic strength and overall ionic strength (as calculated in Geochemist's Workbench). Optimum growth rates were measured when the contribution of Na^+ to ($Na^+ + Mg^{2+}$) ionic strength was above 45% and magnesium concentrations were 1 M or below. When sodium contributed between 20-40% of the ionic strength, rates were more scattered but generally increased with increasing sodium content. Below 20% there was little to no growth. This suggests that, as long as the ratio between Na^+ and Mg^{2+} is acceptable, then growth will occur (Figure 21). The range for chloride was much narrower, with optimum growth occurring when Cl^- made up approximately 45-50% of the ionic strength.

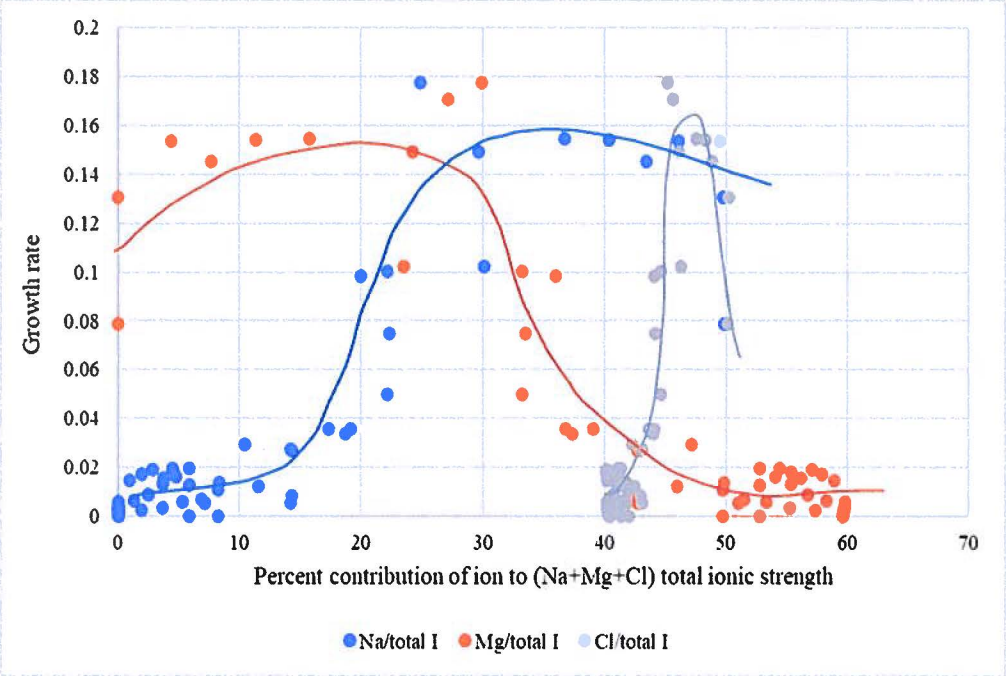


Figure 21. Growth rates of *Halobacterium* sp. as a function of the contribution of Na^+, Mg^{2+} and Cl^- to the sum of their ionic strengths. Trendlines are hand-drawn.

However, this conclusion is too simplistic. Although growth rates were lower as magnesium concentrations increased, the overall extent of growth was still significant at 1.5 M. According to the scale developed by Cray et al. (2013) for chaotropicity/kosmotropicity, NaCl and KCl fall within the kosmotropic range of solutes, while both $MgCl_2$ and $CaCl_2$ are chaotropes. While chaotropes adversely affect the structure and function of cellular macromolecules, kosmotropes have the opposite effect, although the exact mechanism behind this phenomenon is still not

completely understood (Ball and Hallsworth, 2015). This could be a reason for better growth at higher Na^+ concentrations when Mg^{2+} is also relatively high. Others have suggested that ionic composition in general, the divalent to monovalent ion ratio, or the balance of chaotropes to kosmotropes set the limits of habitability (Fox-Powell et al., 2016; Payler et al., 2019; Fisher et al., 2021). These more encompassing explanations appear to support the findings of these experiments better than one parameter alone.

To determine the relative effects of chaotropic and kosmotropic solutes on growth, the ratio of summed chaotropic solute concentrations to summed kosmotropic solute concentrations was calculated for each broth (Appendix B). For ease of graphing, these values were log-normalized. Water activities were graphed as a function of the Log(C/K) values for each broth (Figure 22).

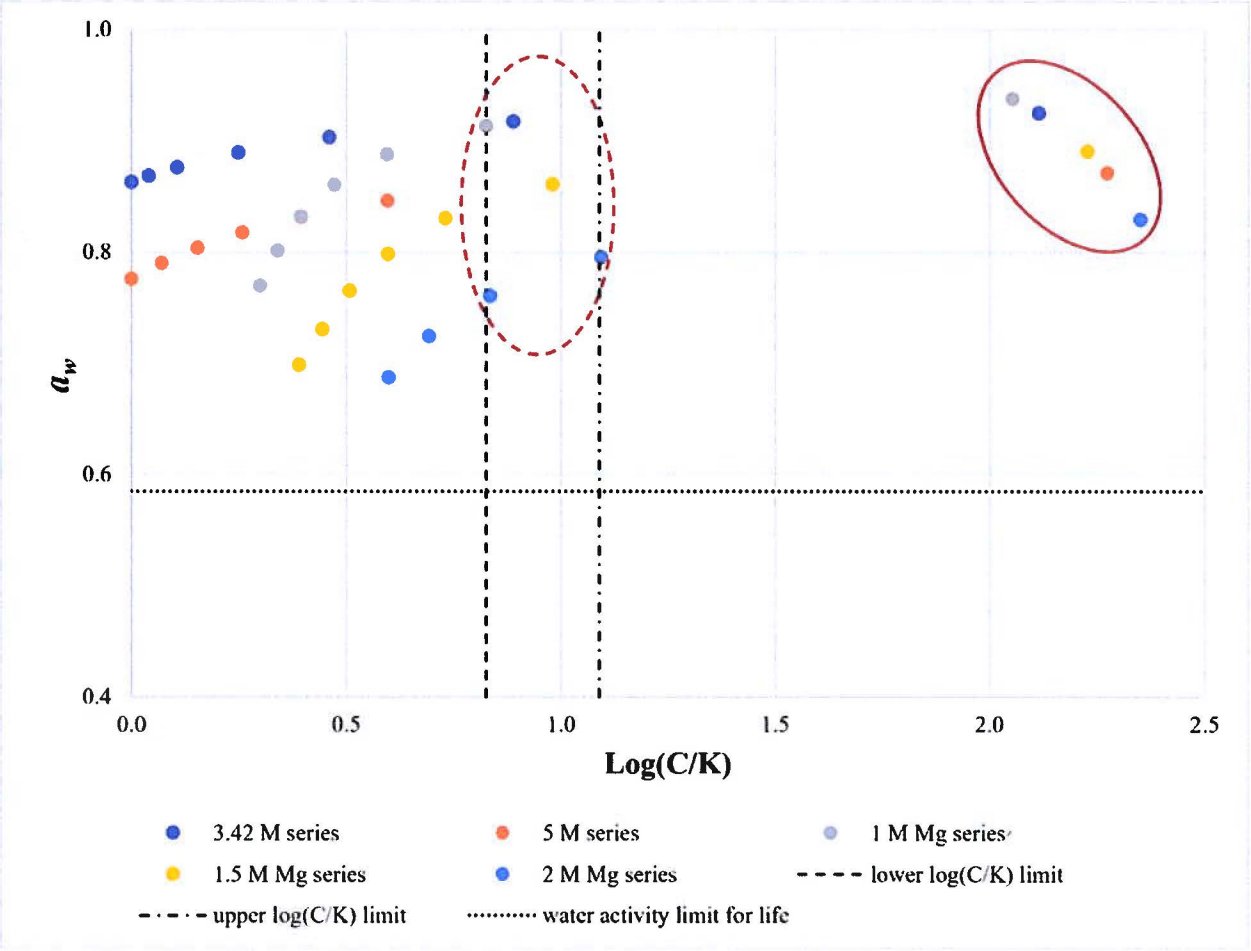


Figure 22. Water activity versus Log(chaotrope/kosmotrope) for all experimental broths. Solid red circle outlines broths in which there was no growth (i.e., broths that contained no sodium). Dashed red circle delineates broths with poor growth (i.e., broths in which $Na^+/ Mg^{2+} < 0.5$).

As shown in Figure 22, the viability of *Halobacterium* sp. is constrained by both water activity and the chaotrope to kosmotrope balance in the broths, suggesting that there is a window delineated by water activity and the Log(C/K) value that may possibly define the limits of a habitable environment. Broths in which no growth occurred are at a significant distance from all others. Broths in which minimal growth occurred fall within a narrow range of log(C/K) values. All broths were above the 0.585 absolute limit of water activity that can sustain life (Stevenson et al., 2017).

Nevertheless, the data do not fit perfectly (see data points within dashed red circle). It appears that the C/K border is not well defined and may be better represented by a range rather than an absolute value, since microbial growth occurred in the 2 M Mg^{2+} medium with 0.5 and 1 M Na^{+} [log(C/K) = 0.796 and 0.836, respectively] but not in 1 M Mg^{2+} broth with 0.5 M Na^{+} (0.826). Although increases in OD in the 2 M Mg^{2+} broth were minimal, the increase in cell numbers was confirmed with plate counts. However, cell splitting and miniaturization (although technically not growth) would still result in an increase in CFU counts, since each "dwarf" cell would theoretically give rise to an individual colony. True reproduction would need to be confirmed by substrate utilization testing.

To test these constraints on other systems, comparisons were extended to other natural terrestrial brines, including those from a German and British salt mine (Figure 23), several surficial hypersaline bodies of water (Figure 24), and numerous deep sea hypersaline anoxic brines (DHABs; Figure 25). Many of these bodies of water are of interest in astrobiological studies that address the possibility of life on Mars. Water activities for all brines were calculated in Geochemist's Workbench and EQ3/6, in order to provide some consistency throughout the data sets (Appendix C). It should be noted that some of the calculated water activities differed significantly from their reported values. In those cases, both values were graphed. Geochemist's Workbench-calculated values are highly dependent upon chloride concentrations. The reported values were, for the most part, obtained using water activity meters that measure the humidity over a specific sample whose free water is at equilibrium with the air above.

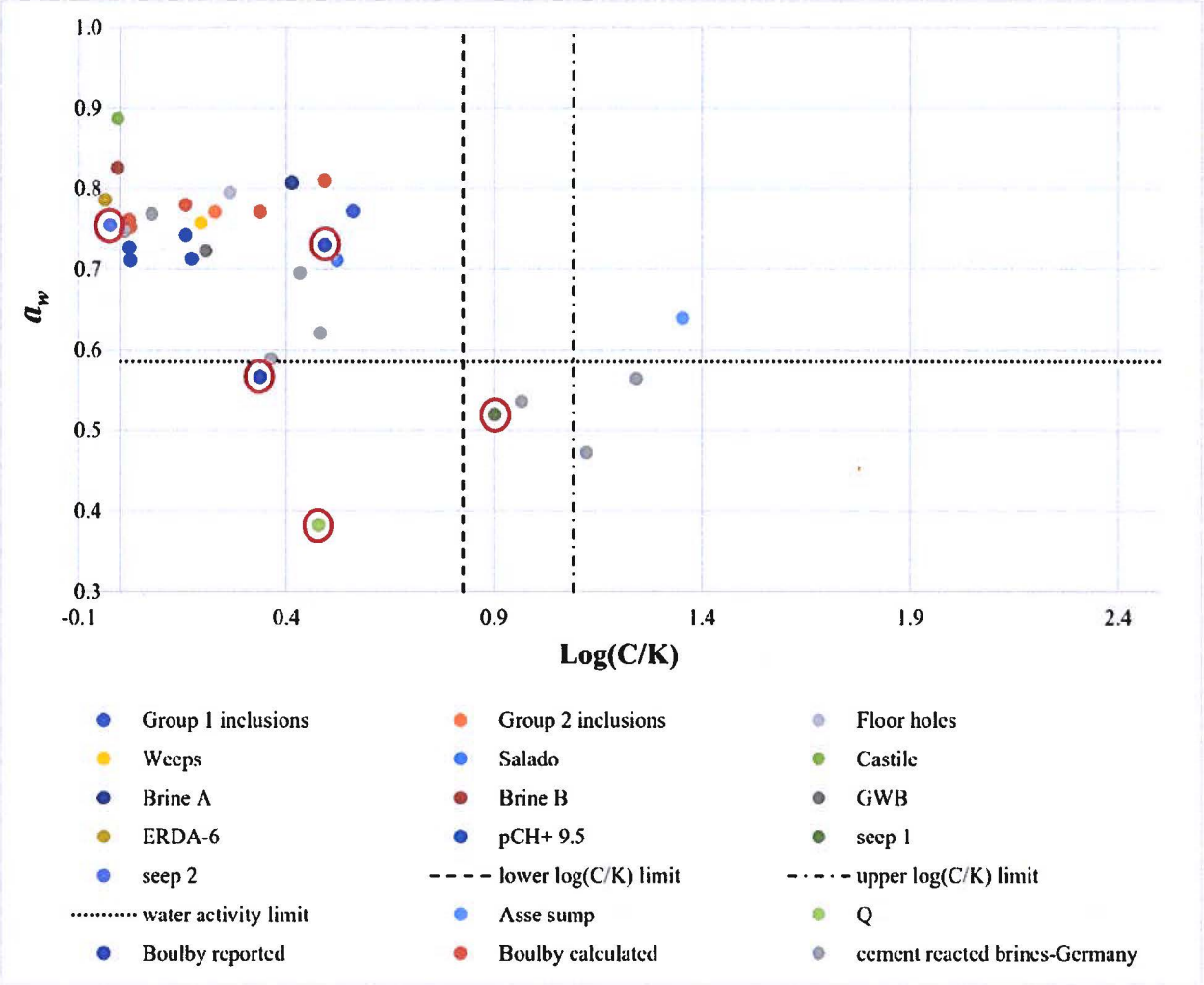


Figure 23. Water activities versus log(C/K) values for subterranean brines. Brines circled in red denote those that were tested for growth and in which no growth occurred. Note: there was a significant difference in the calculated and reported water activity values for the Boulby mine brine in which no growth was observed. See text for more explanation. Not all brines have been tested for growth.

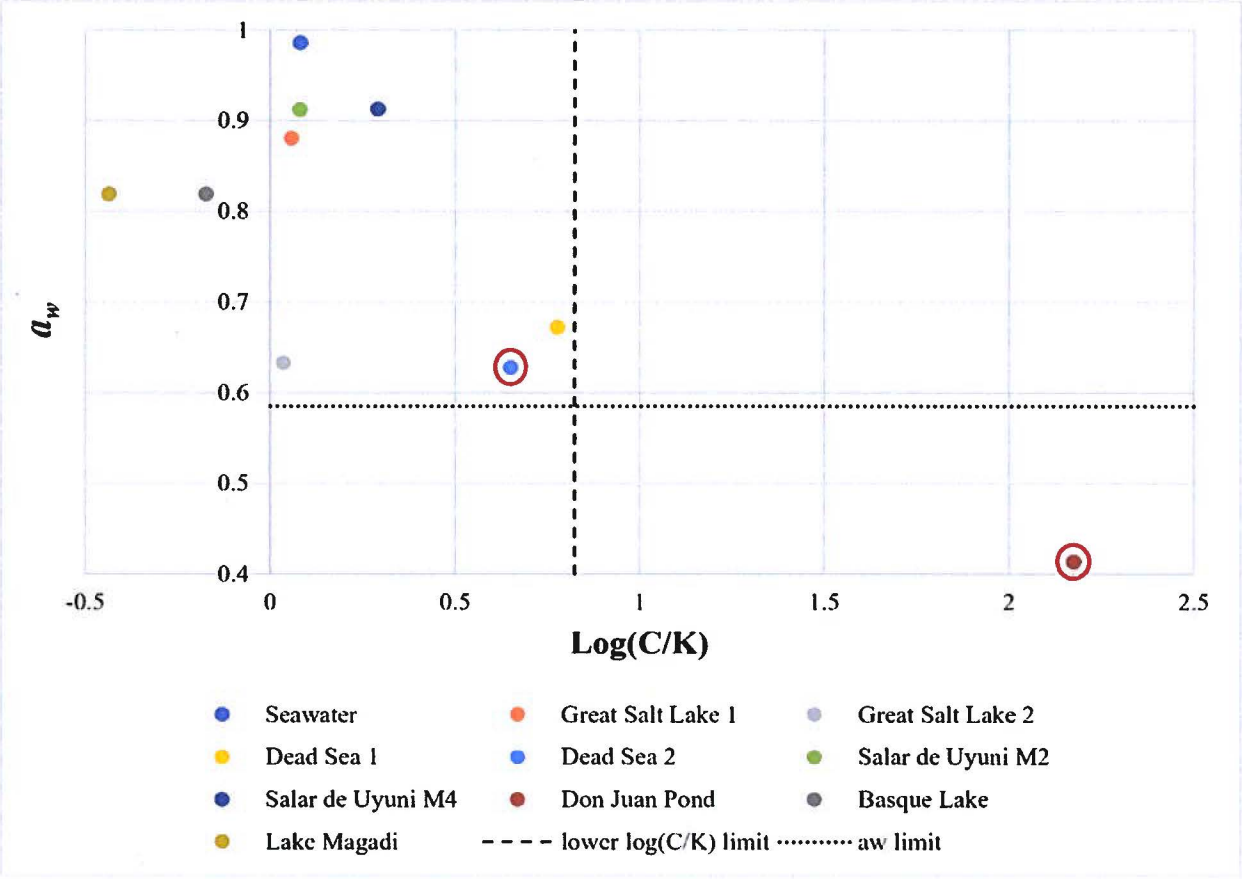


Figure 24. Water activities versus log(C/K) values for surficial brines. Red circles denote brines in which no growth has been shown. Not all brines have been tested for growth.

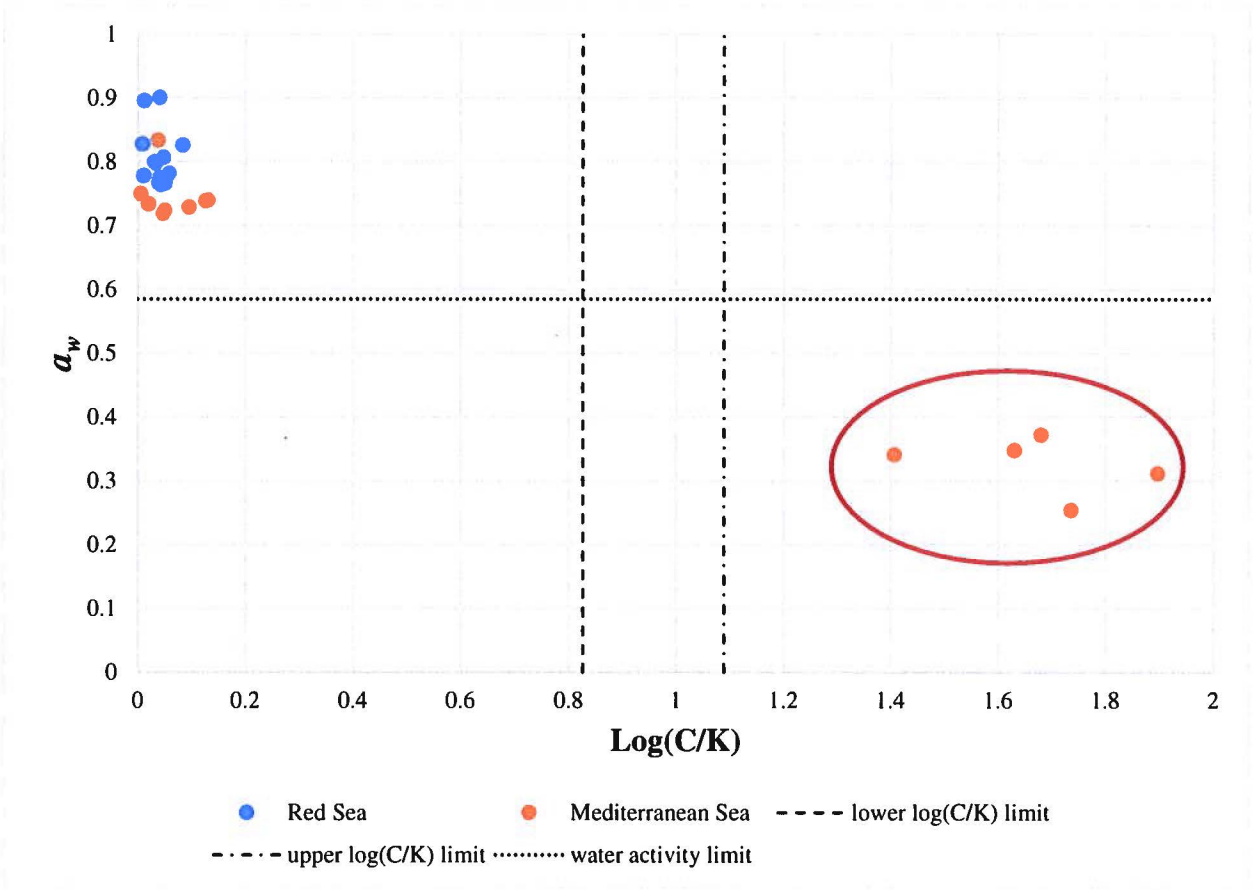


Figure 25. Water activities versus log(C/K) values for deep sea anoxic brines. Red circle denotes athalassohaline brines (i.e., not of marine origin) and therefore dissimilar to WIPP brines.

Results support the window-of-life concept, but they also suggest that an additional constraining factor exists, since some data points appear to fall within the habitability window but their corresponding brines have not been shown to support life (see Figures 23 and 24). Adding pH as an additional constraint to the growth data, the "window" becomes better defined (Figures 26 and 27).

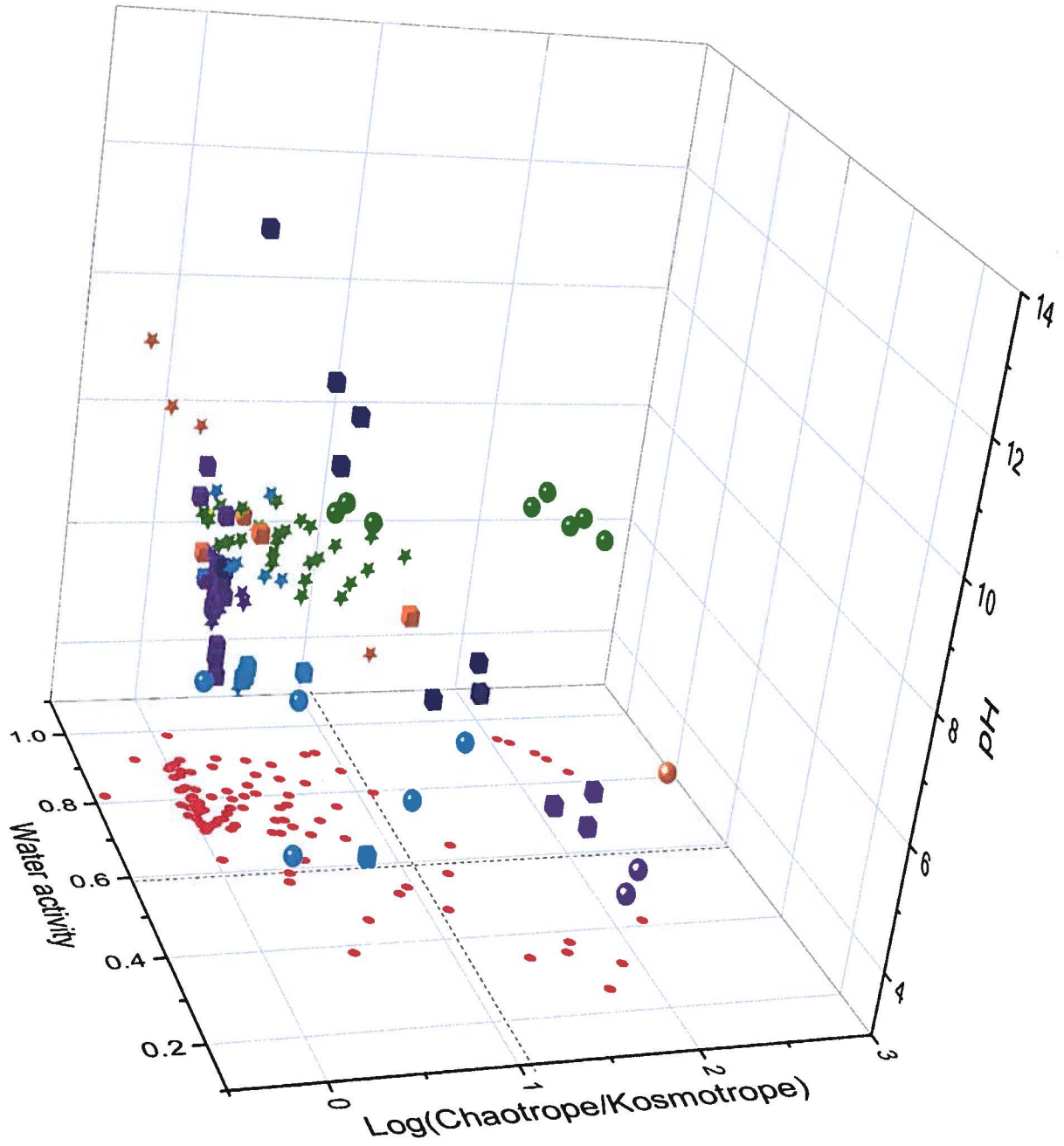


Figure 26. 3D image showing all data points from Appendix C. Red dots are data projected into the x,y plane. Dashed lines mark the upper log(C/K) limit and the water activity limit. For all markers, stars = tested, growth occurred; spheres = tested, no growth occurred; cubes = untested. Green = experimental broths; light blue = subterranean brines; brown = surficial brines; purple = deep sea hypersaline anoxic brines; dark blue = cement/brine experiments.

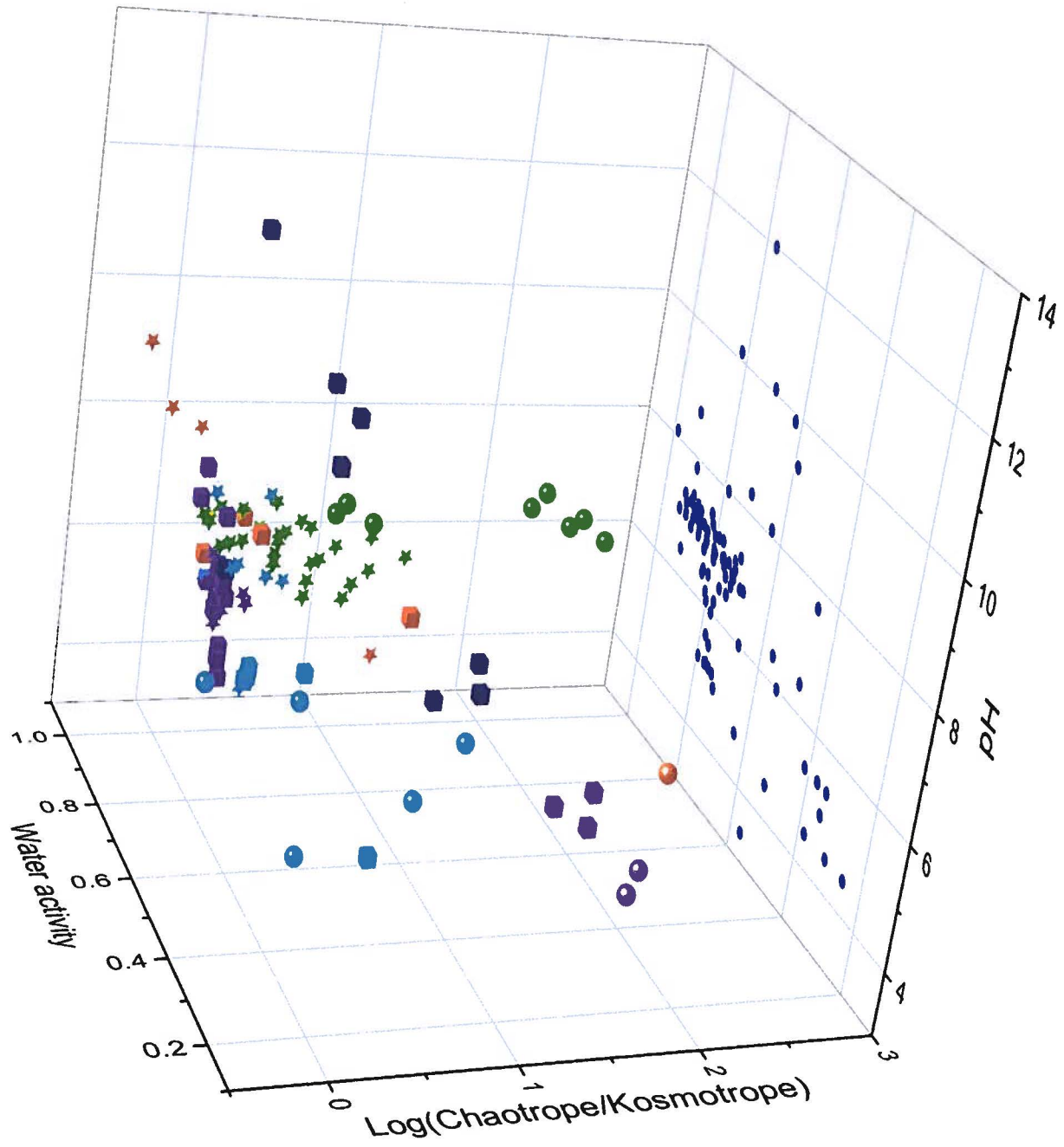


Figure 27. 3D image showing all data points from Appendix C (same as Figure 25). Blue dots are data projected into the z plane.

The green stars appear to cluster near the log(C/K) of zero and above a water activity value of ~0.7. All but one of the measured WIPP brines falls within this delineated zone of habitability. However, growth did not occur in the brine seeps that were tested. In these cases, pH was most likely prohibitive (4.5).

The experiments described in this report were conducted in broth designed to permit microbial growth. WIPP brines contain other salts that were not added to the media, such as lithium chloride and sodium tetraborate. There is little documentation in the literature about the presence of either lithium or borate in other thalassohaline brines. Both are considered chaotropes, and borate is a significant contributor to ionic strength and the high C/K ratio in GWB. Boron is present in seawater and salt evaporite sequences of marine origin. Both boron and lithium are commonly associated with clays in marine and evaporite systems, including WIPP halite (Siegel et al., 1991).

WIPP brines also contain high concentrations of sulfate, which is a kosmotrope that likely has a protective effect on microbial cells. Additionally, the concentrations of calcium and potassium in the broths were much lower than in WIPP brines. *Halobacterium* sp. and other WIPP haloarchaea grow slowly but well in 90-95% strength WIPP brines amended with organics, but complete dissolution of brine and organic components is not readily achieved (Swanson et al., 2013).

Finally, it should also be noted that the pH used in these experiments was slightly lower than those measured for WIPP brines, and more importantly, these experiments were carried out under aerobic conditions. *Halobacterium* sp. prefers circumneutral pH and does not grow well above pH 8.5. pH optima for thalassohaline-derived haloarchaea tend to be between 7-8 and correlate with the sodium concentration of the source environment (Oren, 2006; Bowers and Wiegel, 2011). *Halobacterium* sp., like most haloarchaea, is also an obligate aerobe. There have been no anaerobic extreme halophiles isolated from WIPP halite to date, nor from any other subterranean halites at high ionic strength. However, the presence of extremely halophilic and obligately anaerobic bacteria of the order Halanaerobiales has been discussed previously, since these organisms have been isolated from Culebra groundwaters at the WIPP and DNA signatures have been detected in Gorleben halite. More recently, Halanaerobia have been isolated from a brine stream in a Scottish salt mine in media with 10% (w/v) NaCl (~ 1.71 M; Megaw et al., 2019); thus, their presence at WIPP becomes more probable.

Microbial survival and growth in polyextreme environments are not unheard of. In fact, saturated NaCl is only considered a moderately extreme environment by some (Lee et al., 2018). Many have suggested that organisms present in brines are poly-extremists, capable of survival at high salt and ionic strength and in the presence of high chaotropicity (Hallsworth, 2019). Further, extremes of pH, temperature and pressure can also be found in deep sea hypersaline brines.

That said, a salt deposit such as the Salado Formation is not the equivalent of a natural, biologically active hypersaline body of water. The WIPP repository (and other salt-based nuclear waste repositories), are man-made settings that impose different conditions, and possibly

new stressors, on organisms that might be present. The indigenous and introduced microbial communities may not possess the ability to survive under those imposed conditions. In these experiments, an indigenous extreme halophile was capable of growth in most of the tested media, but it could not grow in all, even if it still survived. It stands to reason that a less halophilic organism will have less chance of survival, let alone growth. Future work may focus on other halophiles and less halophilic organisms and may extend to chaotropic brines containing calcium as the dominant chaotrope, in order to simulate the presence of cementitious wastes.

5.0 QUALITY ASSURANCE, DATA TRACEABILITY AND DOCUMENTATION

All of the data presented in this report, unless specified otherwise, were generated as Quality Level-1 data, in accordance with the WIPP Quality Assurance Program Document. Experiments were performed under the test plan, "Microbial Interactions in the Waste Isolation Pilot Plant" (LCO-ACP-12). Descriptions of the experiments can be found in the scientific notebook, "Characterization of the Microorganisms Indigenous to the WIPP" (ACP-12 Task 1). The following data packages were generated from these experiments:

- *Halobacterium* sp. Water Activity Experiments, Part 1a: Constant Ionic Strength Experiments ICP-MS Data; ACP-2111-01-17-01
- *Halobacterium* sp. Water Activity Experiments, Part 1b: Constant Ionic Strength Experiments IC Data; ACP-2111-01-17-04
- *Halobacterium* sp. Water Activity Experiments, Part 2a: Variable Ionic Strength Experiments ICP-MS Data; ACP-2209-03-09-01
- *Halobacterium* sp. Water Activity Experiments, Part 2b: Variable Ionic Strength Experiments IC Data; ACP-2209-03-09-02

6.0 REFERENCES

Abram D and NE Gibbons. 1961. The Effect of Chlorides of Monovalent Cations, Urea, Detergents, and Heat on Morphology and the Turbidity of Suspensions of Red Halophilic Bacteria. *Canadian Journal of Microbiology* 7: 741-750.

Andrei AS, Banciu HL, Oren A. 2012. Living with Salt: Metabolic and Phylogenetic Diversity of Archaea Inhabiting Saline Ecosystems. *FEMS Microbiology Letters* 330: 1-9.

Antunes A, Olsson-Francis K, McGenity TJ. 2020. Exploring Deep-Sea Brines as Potential Terrestrial Analogues of Oceans in the Icy Moons of the Outer Solar System. *Current Issues in Molecular Biology* 38: 123-162.

Avrahamov N, Antler G, Yechieli Y, Gavrieli I, Joye SB, Saxton M, Turchyn AV, Sivan O. 2014. Anaerobic Oxidation of Methane by Sulfate in Hypersaline Groundwater of the Dead Sea Aquifer. *Geobiology* 12: 511-528.

Ball P and JE Hallsworth. 2015. Water Structure and Chaotropicity: Their Uses, Abuses and Biological Implications. *Physical Chemistry Chemical Physics* 17: 8297-8305.

Bowers KJ, Wiegel J. 2011. Temperature and pH Optima of Extremely Halophilic Archaea: a Mini-Review. *Extremophiles* 15: 119-128.

Broering JM and AS Bommarius. 2008. Kinetic Model for Salt-Induced Protein Deactivation. *The Journal of Physical Chemistry B* 112: 12768-12775.

Cohen S, Shilo M, Kessel M. 1991. Nature of the Salt Dependence of the Envelope of a Dead Sea Archaebacterium, *Haloferax volcanii*. *Archives of Microbiology* 156: 198-203.

Cray JA, Russell JT, Timson DJ, Singhal RS, Hallsworth JE. 2013. A Universal Measure of Chaotropicity and Kosmotropicity. *Environmental Microbiology* 15: 287-296.

Domagalski JL, Orem WH, Eugster HP. 1989. Organic Geochemistry and Brine Composition in Great Salt, Mono, and Walker Lakes. *Geochimica et Cosmochimica Acta* 53: 2857-2872.

Domski PS. 2020. DATA0.FM5: Official Release of the Qualified Pitzer Thermodynamic Database, DATA0.FM5, for EQ3/6 under AP-183, Revision 1. Carlsbad, NM: Sandia National Laboratories. ERMS 572791.

Fendrihan S, Dornmayr-Pfaffenhuemer M, Gerbl FW, Holzinger A, Grösbacher M, Briza P, Erler A, Gruber C, Plätzer K, Stan-Lotter H. 2012. Spherical Particles of Halophilic Archaea Correlate with Exposure to Low Water Activity—Implications for Microbial Survival in Fluid Inclusions of Ancient Halite. *Geobiology* 10: 424-433.

Fisher LA, Pontefract A, Som SM, Carr CE, Klempay B, Schmidt BE, Bowman JS, Bartlett DH. 2021. Current State of Athalassohaline Deep-Sea Hypersaline Anoxic Basin Research—Recommendations for Future Work and Relevance to Astrobiology. *Environmental Microbiology* 23: 3360-3369.

Fox-Powell MG, Hallsworth JE, Cousins CR, Cockell CS. 2016. Ionic Strength is a Barrier to the Habitability of Mars. *Astrobiology* 16: 427-442.

Gramain A, Diaz GC, Demergasso C, Lowenstein TK, McGenity TJ. 2011. Archaeal Diversity along a Subterranean Salt Core from the Salar Grande (Chile). *Environmental Microbiology* 13: 2105-2121.

Grant WD. 2004. Life at Low Water Activity. *Philosophical Transactions of the Royal Society of London* 359: 1249-1267.

Gruber C, Legat A, Pfaffenhuemer M, Radax C, Weidler G, Busse H-J, Stan-Lotter H. 2004. *Halobacterium noricense* sp. nov., an Archaeal Isolate from a Bore Core of an Alpine Permian Salt Deposit, Classification of *Halobacterium* sp. NRC-1 as a Strain of *H. salinarum* and Emended Description of *H. salinarum*. *Extremophiles* 8: 431-439.

Hallsworth JE, Heim S, Timmis KN. 2003. Chaotropic Solutes Cause Water Stress in *Pseudomonas putida*. *Environmental Microbiology* 5: 1270-1280.

Hallsworth JE, Yakimov MM, Golyshin PN, Gillion JLM, D'Auria G, de Lima Alves F, La Cono V, Genovese M, McKew BA, Hayes SL, Harris G, Giuliano L, Timmis KN, McGenity TJ. 2007. Limits of Life in $MgCl_2$-Containing Environments: Chaotropicity Defines the Window. *Environmental Microbiology* 9: 801-813.

Hallsworth JE. 2019. Microbial Unknowns at the Saline Limits for Life. *Nature Ecology & Evolution* 3: 1503-1504.

Jaakkolla ST, Ravantti JJ, Oksanen HM, Bamford DH. 2016. Buried Alive: Microbes from Ancient Halite. *Trends in Microbiology* 24: 148-160.

Kepner, Jr RL and JR Pratt. 1994. Use of Fluorochromes for Direct Enumeration of Total Bacteria in Environmental Samples: Past and Present. *Microbiology Reviews* 58: 603-615.

Kienzler B, Vejmelka P, Herbert H-J, Meyer H, Altenhein-Haese C. 2000. Long-Term Leaching Experiments of Full-Scale Cemented Waste Forms: Experiments and Modeling. *Nuclear Technology* 129: 101-118.

Kimbrel JA, Ballor N, Wu Y-W, David MM, Hazen TC, Simmons BA, Singer SW, Jansson JK. 2018. Microbial Community Structure and Functional Potential Along a Hypersaline Gradient. *Frontiers in Microbiology* 9: 1492.

Lee CJD, McMullan PE, O'Kane CJ, Stevenson A, Santos IC, Roy C, Ghosh W, Mancinelli RL, Mormile MR, McMullan G, Banciu HL, Fares MN, Benison KC, Oren A, Dyall-Smith ML, Hallsworth JE. 2018. NaCl-Saturated Brines are Thermodynamically Moderate, Rather than Extreme, Microbial Habitats. *FEMS Microbiology Reviews* 42: 672-693.

Lucchini J-F, Borkowski M, Khaing H, Richmann MK, Swanson J, Simmons K, Reed DT. 2013. WIPP Actinide-Relevant Brine Chemistry. Report LCO-ACP-15. Los Alamos National Laboratory; Carlsbad, NM.

Marion GM, Fritsen CH, Eicken H, Payne MC. 2003. The Search for Life on Europa: Limiting Environmental Factors, Potential Habitats, and Earth Analogues. *Astrobiology* 3: 785-811.

Megaw J, Kelly SA, Thompson TP, Skvortsov T, Gilmore BF. 2019. Profiling the Microbial Community of a Triassic Halite Deposit in Northern Ireland: an Environment with Significant Potential for Biodiscovery. *FEMS Microbiology Letters* 366: doi: 10.1093/femsle/fnz242.

Mohr V and H Larsen. 1963. On the Structural Transformation and Lysis of *Halobacterium salinarum* in Hypotonic and Isotonic Solutions. *Journal of General Microbiology* 31:267-280.

Oren A. 2006. Life at High Salt Concentrations. In: Falkow S, Rosenberg E, Schleifer K-H, Stackebrandt E, Dworkin M, editors. The Prokaryotes. New York: Springer. pp. 263-282.

Park JS, Vreeland RH, Cho BC, Lowenstein TK, Timofeeff MN, Rosenzweig WD. 2009. Haloarchaeal Diversity in 23, 121 and 419 MYA Salts. *Geobiology* 7: 515-523.

Payler SJ, Biddle JF, Sherwood Lollar B, Fox-Powell MG, Edwards T, Ngwenya BT, Paling SM, Cockell C. 2019. An Ionic Limit to Life in the Deep Subsurface. *Frontiers in Microbiology* 10: Article 426. doi: 10.3389/fmicb.2019.00426.

Radax C, Gruber C, Stan-Lotter H. 2001. Novel Haloarchaeal 16S rRNA Gene Sequences from Alpine Permo-Triassic Rock Salt. *Extremophiles* 5: 221-228.

dC Rubin SS, Marín I, Gómez MJ, Morales EA, Zekker I, San Martín-Uriz P, Rodríguez N, Amils R. 2017. Prokaryotic Diversity and Community Composition in the Salar de Uyuni, a Large Scale, Chaotropic Salt Flat. *Environmental Microbiology* 19: 3745-3754.

Siegel MD, Robinson KL, Myers J. 1991. Solute Relationships in Groundwaters from the Culebra Dolomite and Related Rocks in the Waste Isolation Pilot Plant Area, Southeastern New Mexico. Report SAND88-0196. Sandia National Laboratories; Albuquerque, NM.

Stein CL and JL Krumhansl. 1986. Chemistry of Brines in Salt from the Waste Isolation Pilot Plant (WIPP), Southeastern New Mexico: A Preliminary Investigation. Report SAND85-0897. Sandia National Laboratories; Albuquerque, NM.

Stevenson A, Cray JA, Williams JP, Santos R, Sahay R, Neuenkirchen N, McClure CD, Grant I, Houghton JDR, Quinn JP, Timson DJ, Patil SV, Singhal S, Antón J, Dijksterhuis J, Hocking AD, Lievens B, Rangel DEN, Voytek MA, Gunde-Cimerman N, Oren A, Timmis KN, McGenity TJ, Hallsworth JE. 2014. Is there a Common Water Activity Limit for the Three Domains of Life? *The ISME Journal* 1-19.

Stevenson A, Hamill PG, O'Kane CJ, Kminek G, Rummel JD, Voytek MA, Dijksterhuis J, Hallsworth JE. 2017. *Aspergillus penicillioides* Differentiation and Cell Division at 0.585 Water Activity. *Environmental Microbiology* 19: 687-697.

Swanson J, Simmons K, Norden D, Ams D, Reed D. 2012. Status Report on the Microbial Characterization of Halite and Groundwater Samples from the WIPP. LA-UR-12-22824. Los Alamos National Laboratory; Carlsbad, NM.

Swanson J, Simmons K, Norden D, Ams D, Reed D. 2012b. Status Report on the Microbial Characterization of Halite and Groundwater Samples from the WIPP. Report LCO-ACP-12. Los Alamos National Laboratory; Carlsbad, NM.

Swanson JS, Norden DM, Khaing HM, Reed DT. 2013. Degradation of Organic Complexing Agents by Halophilic Microorganisms in Brines. *Geomicrobiology Journal* 30: 189-198.

Swanson J and D Reed. 2018. Update on Microbiology Research for the Waste Isolation Pilot Plant. Report LA-UR 18-31313. Los Alamos National Laboratory; Carlsbad, NM.

Swanson J. 2019. Review of the Microbial Colloid Contribution to the WIPP Actinide Source Term. Report LCO-ACP-23. LA-UR 19-22310. Los Alamos National Laboratory; Carlsbad, NM.

Thies A, Schultze JW. 1996. Corrosion and Passivity of Hastelloy C4 in a High Salinity Brine. *Materials and Corrosion* 47: 146-153.

van der Wielen PWJJ, Bolhuis H, Borin S, Daffonchio D, Corselli C, Giuliano L, D'Auria G, de Lange GJ, Huebner A, Varnavas SP, Thomson J, Tambuuini C, Marty D, McGenity TJ, Timmis KN, BioDeep Scientific Party. 2005. The Enigma of Prokaryotic Life in Deep Hypersaline Anoxic Basins. *Science* 307: 121-123.

Vreeland RH, Piselli Jr AF, McDonnough S, Meyers SS. 1998. Distribution and Diversity of Halophilic Bacteria in a Subsurface Salt Formation. *Extremophiles* 2: 321-331.

Vreeland RH, Jones J, Monson A, Rosenzweig WD, Lowenstein TK, Timofeeff M, Satterfield C, Cho BC, Park JS, Wallace A, Grant WD. 2007. Isolation of live Cretaceous (121-112 million years old) halophilic *Archaea* from primary salt crystals. *Geomicrobiology Journal* 24: 275-282.

Williams JP and JE Hallsworth. 2009. Limits of Life in Hostile Environments: No Barriers to Biosphere Function? *Environmental Microbiology* 11: 3292-3308.

Wolery TJ. 1992. EQ3/6, A Software Package for Geochemical Modeling of Aqueous systems: Package Overview and Installation Guide. Version 7.0. Lawrence Livermore National Laboratory; Livermore, CA.

Yakimov MM, La Cono V, Spada GL, Bortoluzzi G, Messina E, Smedile F, Arcadi E, Borghini M, Ferrer M, Schmitt-Kopplin P, Hertkorn N, Cray JA, Hallsworth JE, Golyshin PN, Giuliano L. 2015. Microbial Community of the Deep-Sea Brine Lake Kryos Seawater-Brine Interface is Active Below the Chaotropicity Limit of Life as Revealed by Recovery of mRNA. *Environmental Microbiology* 17: 364-382.

Yildiz E, Ozcan B, Caliskan M. 2012. Isolation, Characterization and Phylogenetic Analysis of Halophilic Archaea from a Salt Mine in Central Anatolia (Turkey). *Polish Journal of Microbiology* 61: 111-117.

Zirnstein I and T Arnold. 2015. Insights into the Biodiversity of Salt Sumps in the Asse II Salt Mine, Germany. *In* Proceedings of the Third International Workshop on Actinide and Brine Chemistry in a Salt-Based Repository (ABC-Salt III). Reed D, Altmaier M, eds.

APPENDIX A. Growth rates calculated during exponential growth; maximum optical density values.

BROTH ID	[NaCl], M	[$MgCl_2$], M	Growth Rate (day^{-1}) during Exponential Phase (days used)	Extent of Growth, as Maximum OD (day reached)
3.42-A	3.42	0	0.1308 (2-4)	0.522 (7)
3.42-B	3.12	0.1	0.1538 (2-4)	0.570 (8)
3.42-C	2.67	0.25	0.1540 (2-4)	0.507 (8)
3.42-D	1.92	0.5	0.1023 (2-4)	0.370 (8)
3.42-E	1.17	0.75	0.0355 (2-4)	0.191 (8)
3.42-F	0.42	1	0.0052 (2-4)	0.030 (5)
3.42-G	0	1.15	0 (2-4)	0.012 (6)
5-A	5	0	0.1132 (3-6)	0.520 (7)
5-B	4.25	0.25	0.1453 (2-4)	0.507 (6)
5-C	3.5	0.5	0.1547 (2-4)	0.504 (6)
5-D	2.75	0.75	0.1492 (2-4)	0.503 (6)
5-E	2	1	0.0891 (5-8)	0.486 (9)
5-F	1.25	1.25	0.0305 (1-3)	0.121 (8)
5-G	0.5	1.5	0.0015 (2-4)	0.030 (5)
5-H	0	1.67	0.0018 (2-4)	0.022 (7)
1-A	0	1	0 (2-4)	0.006 (1)
1-B	0.5	1	0 (2-4)	0.035 (8-9)
1-C	1	1	0.0275 (2-4)	0.130 (9)
1-D	1.5	1	0.0335 (2-4)	0.307 (9)
1-E	2	1	0.1003 (2-4)	0.671 (10)
1-F	2.5	1	0.1777 (2-4)	0.586 (7)
1-G	3	1	0.1707 (2-4)	0.533 (7)
1.5-A	0	1.5	0.0018 (2-4)	0.018 (11)
1.5-B	0.5	1.5	0.0129 (1-4)	0.075 (11)
1.5-C	1	1.5	0.0295 (1-3)	0.178 (11)
1.5-D	1.5	1.5	0.0268 (1-3)	0.173 (11)
1.5-E	2	1.5	0.0358 (2-5)	0.512 (14)
1.5-F	2.5	1.5	0.0983 (3-6)	0.493 (8)
1.5-G	3	1.5	0.0746 (4-8)	0.452 (11)
2-A	0	2	0.0038 (1-3)	0.033 (15)
2-B	0.5	2	0.0197 (1-3)	0.119 (21)
2-C	1	2	0.0135 (1-3)	0.087 (21)
2-D	1.5	2	0.0107 (1-3)	0.065 (21)
2-E	2	2	0.0083 (1-3)	0.178 (21)

APPENDIX B. Values for Log(C/K) and water activities for all experimental broths.

BROTH ID	Log(C/K)	Calculated Water Activity	
		Geochemist's Workbench	EQ3/6
3.42-A	0.0006	0.8632	0.8572
3.42-B	0.0401	0.8684	0.8620
3.42-C	0.1071	0.8761	0.8694
3.42-D	0.2487	0.8895	0.8821
3.42-E	0.4600	0.9032	0.8955
3.42-F	0.8891	0.9176	0.9091
3.42-G	2.1149	0.9251	0.9166
5-A	0.0004	0.7762	0.7766
5-B	0.0706	0.7900	0.7882
5-C	0.1543	0.8039	0.7999
5-D	0.2581	0.8177	0.8119
5-E	0.3949	0.8317	0.8243
5-F	0.5956	0.8462	0.8374
5-G	0.9800	0.8612	0.8512
5-H	2.2744	0.8711	0.8605
1-A	2.0535	0.9380	0.9313
1-B	0.8263	0.9136	0.9056
1-C	0.5940	0.8878	0.8792
1-D	0.4724	0.8606	0.8521
1-E	0.3949	0.8319	0.8243
1-F	0.3403	0.8015	0.7960
1-G	0.2994	0.7696	0.7672
1.5-A	2.2281	0.8903	0.8804
1.5-B	0.9800	0.8611	0.8512
1.5-C	0.7313	0.8306	0.8215
1.5-D	0.5966	0.7986	0.7915
1.5-E	0.5082	0.7654	0.7612
1.5-F	0.4445	0.7307	0.7307
1.5-G	0.3907	0.6984	0.7090
2-A	2.3523	0.8294	0.8184
2-B	1.0934	0.7955	0.7865
2-C	0.8356	0.7606	0.7545
2-D	0.6931	0.7244	0.7226
2-E	0.5980	0.6873	0.6909

APPENDIX C. Values for log(chaotrope/kosmotrope) and calculated water activities for various terrestrial brines.

BRINE	LOG(C/K)	*Calculated a_w GWB, EQ3/6 (Reported)	REFERENCE FOR BRINE COMPOSITION
Subterranean Brines			
WIPP:			
GWB	0.206	0.722†, 0.736 (NR)	Lucchini et al., 2013
ERDA	-0.037	0.786, 0.787 (NR)	
pC_{H+} 9.5	0.171	0.727, 0.732 (NR)	
Group 1 fluid inclusions	0.559	0.772, 0.770 (NR)	Stein and Krumhansl, 1986
Group 2 fluid inclusions	0.229	0.771, 0.767 (NR)	
Floor holes	0.265	0.795, 0.772 (NR)	
Weeps	0.195	0.757, 0.756 (NR)	
Brine A	0.414	0.807, 0.805 (NR)	
Brine B	-0.006	0.826, 0.821 (NR)	
WIPP seep 1	0.902	NC†, 0.509	Unpublished analysis
WIPP seep 2	-0.025	0.755, NC	
German salt mines:			
Q	0.478	0.382, 0.669, (NR)	Thies and Schulze, 1996
Asse sump fluid	1.355	0.437, 0.523, (NR)	Zirnstein and Arnold, 2015
Boulby salt mine brines (UK):			Payler et al., 2019
Billingham	0.021	0.761, 0.749 (0.727)	
215	0.024	0.752, 0.739 (0.711)	
29XC	0.492	0.811, 0.696 (0.730)	
44XC	0.157	0.782, 0.770 (0.742)	
101-P	0.338	0.771, 0.827 (0.566)	
Surficial Brines			
Dead Sea	0.780	0.670, 0.663 (0.670)	Avrahamov et al., 2014
	0.653	0.628, 0.642 (0.690)	Yakimov et al., 2015
Great Salt Lake (GSL)	0.059	0.881, 0.870 (0.750)	Domagalski et al., 1989
	0.036	0.633, 0.749 (0.69)	Marion et al., 2003
Salar de Uyuni-M2 (Bolivia)	0.081	NC, NC (0.912)	dC Rubin et al., 2017
Salar de Uyuni-M4	0.292	NC, NC (0.913)	
Don Juan Pond (Antarctica)	2.176	0.176, 0.294 (0.414)	Marion et al., 2003
Basque Lake (Canada)	-0.173	0.819, 0.895 (0.919)	
Lake Magadi (Kenya)	-0.409	0.819, 0.708 (0.819)	
Seawater	0.081	0.986, 0.975 (0.981)	Van der Wielen et al., 2005
Deep Hypersaline Anoxic Brines (DHABs)			
Mediterranean Sea:			
L'Atalante	0.048	0.719, NC, (NR)	Antunes et al., 2020; Yakimov et al., 2015
Bannock	0.131	0.778, 0.743 (NR)	
Urania	0.038	0.834, 0.841 (NR)	
Discovery	1.736	0.264, 0.370, (0.382)	
Hephaestus	1.631	0.348, 0.402 (0.395)	
Kryos	1.680	0.341, 0.427 (0.399)	
Thetis	0.051	0.724, NC, (NR)	
Tyro	0.007	0.750, 0.756, (NR)	
L'Atalante	0.021	0.734, NC, (NR)	van der Wielen et al., 2005
Bannock	0.127	0.739, 0.746, (NR)	
Discovery	1.897	0.312, 0.392 (NR)	
Urania	0.038	0.834, 0.841, (NR)	

Red Sea:			
Albatross	0.033	0.798, 0.797, (NR)	Antunes et al., 2020; Fisher et al., 2021
Atlantis II	0.051	0.766, 0.765, (NR)	
Chain	0.043	0.764, 0.766, (NR)	
Conrad	0.032	0.800, 0.793, (NR)	
Discovery	0.041	0.775, 0.776, (NR)	
Erba	0.013	0.896, 0.890, (NR)	
Kebrit	0.039	0.767, 0.769, (NR)	
Nereus	0.084	0.826, 0.823, (NR)	
Oceanographer	0.059	0.782, 0.794, (NR)	
Port Sudan	0.009	0.838, 0.834, (NR)	
Shaban	0.012	0.778, 0.781, (NR)	
Suakin	0.041	0.901, 0.895, (NR)	
Valdivia	0.048	0.807, 0.789, (NR)	
Reference Brines			
5 M NaCl	0.000	0.778	Unpublished
2.3 M $MgCl_2$	Technically undefined, but with 1 mM kosmotropes = 3.839	0.788	Hallsworth et al., 2007; reported limit for life in the absence of compensating kosmotropes

*Water activities calculated in GWB cannot be considered QL-1 data, since the software has not been officially qualified. Compare to EQ3/6 calculations. This database is qualified; however, it does not contain all ions of interest.
NC = Not Calculated:
Salar de Uyuni—no Li^+ in EQ3/6 database
WIPP seep #2, LAtalante, Thetis—no pH values
†cannot calculate in GWB with full strength borate concentration (Generic Weep Brine calculated using quarter borate concentration)
NR = Not Reported